



People's Democratic Republic of Algeria  
Ministry of Higher Education and Scientific Research



**University Amar Thelidji- Laghouat**  
**Faculty of Technology**  
**Department of Process Engineering**

# MASTER'S MANUSCRIT

Presented by:

**BENCHINE Noussaiba**

**MECHEMACHE Khadidja**

**DOMAIN: Sciences and Technologies**

**Branch: Process Engineering**

**MAJOR: Chemical Engineering**

This work is entitled:

**Pressure-Volume (PV) Diagrams plotting, using Cubic Equations of States (EOS), for pure substance, and some thermodynamic properties calculations**

Supervisory and examining committee:

First and last name	Grade	Quality
Mr. TAOUTI Mohammed Benabdallah	Full Professor.	President
Mr. TAOUTI Mohammed Bachir	Assist. Lect. A.	Examiner
Mr. BOUREZG Mohammed Tahar	Assist. Lect. A	Supervisor

**Promotion: JUNE 2025**

## *Acknowledgment*

*First and foremost, all praise and gratitude are due to Allah Almighty, whose boundless grace, mercy, and guidance granted us the strength, patience, and perseverance to bring this work to completion.*

*This research project was carried out within the Process Engineering Department at the University of Laghouat Amar Telidji, an environment that has greatly contributed to our academic and personal development.*

*We would like to express our deepest appreciation to our supervisor, Dr. BOUREZG Mohammed Tahar, for his invaluable mentorship, constructive feedback, and constant encouragement. His scientific insight and human support were essential at every stage of this thesis.*

*We are also sincerely thankful to the members of the jury, Mr. President and Mr. Examiner, for devoting their time to evaluate this work and for their thoughtful remarks and suggestions.*

*For the last, we would like to thank our fellow students, friends, and all those near or far who supported, encouraged, and believed in us during the course of this work. Your presence made this journey more meaningful and rewarding.*

## *Dedication*

*To my beloved father may God have mercy on him. Not a day passes without the ache of your absence in my heart. my soul longs for your presence, your smile, your proud gaze. I wish with all my being that you were here to share this moment with me. Your memory lives on in every step I take, and the love I hold for you is beyond what words could ever express. You are deeply missed, eternally cherished, and forever loved.*

*To my beloved mother, whose strength and grace have shaped the person I am today your endless support, and tireless sacrifices have been the pillars of my journey. You have stood by me with unwavering faith, and your blessings have lit my path through every step. I can never truly express how much your presence has meant to me, nor fully repay the love and care you've given so selflessly.*

*To my dear brothers and sisters, your unwavering support and constant encouragement have been a true source of strength for me. I am deeply grateful for the love, faith, and motivation you've given me along the way. From the bottom of my heart, I love you all more than can you imagine.*

*To my dearest friends, I am endlessly grateful for the gift of your friendship. You have been by my side through both joyful moments and the hardest of days. The memories we've shared together over the years are etched in my heart forever. Your presence in my life is a blessing beyond words. I love you all deeply.*

*Last but not least, I want to thank me. I am truly proud of how far I've come, I'm deeply grateful to God for all His blessings. This journey hasn't been easy, but I've kept going and for that. I pray for even more success, growth, and happiness in my life.*

*Benchine Noussaiba*

## *Dédication*

*Je dédie ce travail à toutes les personnes qui m'ont accompagné de près ou de loin durant cette étape importante de ma vie.*

*À ma **mère**, pour son amour, ses prières et sa tendresse infinie. Merci d'avoir toujours cru en moi.*

*À mon **père**, pour sa présence rassurante, son soutien constant et son amour silencieux.*

*À ma **famille bien-aimée**, pilier de ma réussite, merci pour votre amour, votre patience et vos sacrifices. Vos prières et votre confiance en moi m'ont donné la force d'avancer même dans les moments les plus difficiles.*

*À mes **amis fidèles**, pour leur soutien moral, leurs encouragements, leurs conseils, mais aussi pour les moments de joie, de rire et de motivation partagée. Votre présence a été essentielle pour alléger le poids du parcours.*

*À mon **encadrant**, pour son encadrement de qualité, sa disponibilité, sa bienveillance et ses conseils constructifs qui m'ont permis d'avancer dans ce travail avec rigueur et confiance.*

*Et tout particulièrement à mon **frère Samir**, merci pour ta patience, ton aide précieuse et ta présence constante à mes côtés. Ton soutien m'a été inestimable et restera gravé dans ma mémoire.*

*À toutes ces personnes, je dis du fond du cœur : **merci**.*

**MECHEMACHE Khadidja**

## *List of abbreviations & symbols*

EOS: Equation of state.

Hr: Residual enthalpy

NIST: National Institute of Standards and Technology.

Pc: Critical pressure.

PR: Peng-Robinson.

Pr: Reduced pressure.

P-T: Pressure- temperature.

P-V: Pressure-molar volume

PVT: Pressure-molar volume-temperature.

RMSE: Root Mean Squared Error.

SRK: Soave-Redlich-Kwong.

Tc: Critical temperature.

Tc: Critical temperature.

Tr: Reduced temperature.

Vc: Critical molar volume.

VdW: Van der Waals.

VLE: Vapor-liquid equilibrium.

Zc: Critical compressibility factor

$\omega$ : Acentric Factor.

$\varphi$ : fugacity coefficient.

## Table of figures

Figure I-1:Constant-pressure change from liquid to vapor phase for a pure substance .....	6
Figure I-2:Typical phase transition diagram for pure compounds. ....	7
Figure I-3:Phase diagram of carbon monoxide (CO <sub>2</sub> ) showing the gas (G), the liquid (L) and solid (S) phases.....	8
Figure I-4:The PV graph of pure fluid (the solid phase is not shown).....	9
Figure I-5:The PV graph of pure fluid with showing the isotherm of the ideal gas. ....	12
Figure II-1:Experimental PV diagram plotting for ethylene.....	26
Figure II-2:Calculation of SRK parameters.....	27
Figure II-3:Initial estimate of $P_{\text{sat}}$ .....	27
Figure II-4: Iterative Calculation of the parameters .....	27
Figure II-5:Iteration parametrs.....	28
Figure II-6:The main iteration of fugacity coefficient.....	28
Figure II-7:Numerical Resolution of the SRK Cubic Equation .....	29
Figure II-8:Fugacity coefficients calculation. ....	31
Figure II-9:Numerical derivative for the fugacitys .....	31
Figure II-10: Residual Enthalpy Calculation for Vapor Phase Using SRK EOS. ....	33
Figure II-11:PV diagram of the calculation and experimental results.....	35
Figure II-12:PV diagram of the calculation and experimental results for PR. ....	40

## *List of Tables*

Table II-1:Results of calculation the saturation pressure.....	34
Table II-2: Results of calculation the compressibility factor and molar volume. ....	36
Table II-3:Results of calculation the residual enthalpy.....	37
Table II-4:Results of calculation the saturation pressure with PR .....	39
Table II-5:Results of calculation the molar volume with PR.....	41
Table II-6:Results of calculation the residual enthalpy and the enthalpy of vaporization with PR. ....	42
Table II-7: RMSE results for the saturation pressure of ethylene. ....	43
Table II-8: Results of RMSE calculation for the molar volume of ethylene with SRK EOS...44	
Table II-9:Results of RMSE calculation for the molar volume of ethylene with SRK EOS....45	
Table II-10:Results of RMSE calculation for the enthalpy of vaporization of ethylene. ....46	
Table II-11:Comparative Performance of SRK and PR Equations of State for Key Thermodynamic Properties.....	48

## ***Table of Contents***

*List of abbreviations & symbols*

*Table of figures*

*List of Tables*

*General Introduction* ..... 4

*CHAPTER I: PVT Behavior for VLE for pure fluid and the importance of equation of state.* ..... 4

I.1. Introduction .....5

I.2. Phase Equilibrium in a pure substance. ....6

I.3. P-V-T Behavior of Real Compounds.....7

I.4. PV Graph.....8

I.5. Equilibrium Conditions at Constant T & P .....10

I.6.PVT Behavior of low & moderate density gases. ....11

I.7. Compressibility Factor.....12

I.8. Cubic Equations of State.....13

I.8.1. Van der Waals Equation. ....14

I.8.2 Soave Redlich Kwong Equation.....15

I.8.3. Peng Robinson Equation. ....16

I.9.Saturation Pressure Determination .....16

I.9.1. Methods of calculation the Saturation Pressure .....17

I.10.Vaporization Enthalpy Calculation Procedure .....21

I.11. Root Mean Squared Error .....23

*CHAPTER II: Interpretation and evaluation the results of calculation* ..... 24

II.1. Introduction.....25

II.2. Experimental data of ethylene from NIST.....26

II.3. Experimental PV diagram of ethylene from NIST.....26

II.4.SRK EOS Performances Evaluation .....26

II.5.PR EOS Performances Evaluation. ....37

II.6. Results of RMSE calculation. ....42

*General Conclusion* ..... 49

*Bibliography*

*Appendix*

# *General Introduction*

Vapor-Liquid Equilibrium (VLE) is a fundamental concept in thermodynamics and chemical engineering that describes distribution of chemical species between vapor and liquid phases at equilibrium. This equilibrium occurs when the rates of evaporation and condensation for each component in the system are balanced, resulting in no net transfer of matter between phases. VLE is governed by the principle that chemical potential of each component must be equal in both phases. Understanding VLE is critical for designing and optimizing separation processes such as distillation, absorption, and extraction, which are ubiquitous in industries like petroleum refining, chemical manufacturing, and environmental engineering.

To model such behavior, Equations of State (EOS) are employed. These mathematical formulations are essential tools in predicting thermodynamic properties such as fugacity, enthalpy, and entropy. The simplest EOS is the Ideal Gas Law, which assumes no intermolecular forces and negligible molecular volume. However, real fluids deviate from ideal behavior, especially at high pressures and near critical conditions, necessitating more sophisticated models like the Soave–Redlich–Kwong (SRK) and Peng–Robinson (PR) equations. These cubic EOS incorporate parameters to account for molecular interactions, enabling more accurate predictions of phase behavior for pure substances. Cubic EOS can be used to generate phase diagrams, determine saturation pressure, and evaluate other key thermodynamic properties. One widely adopted method for estimating saturation pressure involves equating the fugacity coefficients of the liquid and vapor phases. This approach allows accurate determination of equilibrium conditions without requiring extensive experimental data.

Numerous studies have explored accuracy and limitations of cubic EOS in modeling vapor-liquid equilibrium of pures and mixtures. Soave (1972) introduced a modification to the Redlich-Kwong equation to improve vapor pressure predictions, leading to SRK model. Peng and Robinson (1976) proposed an equation, designed to enhance predictions of both vapor pressure and liquid density. Despite their widespread use, variations in performance depending on the fluid type and conditions continue to drive studies that validate and compare these models against experimental benchmarks, such as those provided by the NIST database. These efforts are especially important for reactive compounds like ethylene, a light hydrocarbon that plays a vital role in the petrochemical industry. Its high chemical reactivity in addition reactions, coming from its carbon double bond (C=C), particularly  $\pi$  bond. This property is widely exploited in industry, especially in the production of polyethylene (PE), one of the most used plastics. Ethylene's reactivity and central role in petrochemical processes make it a key compound requiring accurate thermodynamic modeling.

Considering these aspects, our research is focused on evaluating the performance of the SRK and PR EOS in predicting key thermodynamic properties of ethylene. Specifically, we assess their ability to calculate saturation pressure, compressibility factors, and molar volumes across a range of temperatures. Another key property investigated in this work is the enthalpy of vaporization ( $\Delta H_{\text{vap}}$ ), which is essential in energy balance calculations and thermal system design, influencing equipment sizing, safety analysis, and process efficiency. EOS models can be used not only to predict phase compositions but also to evaluate  $\Delta H_{\text{vap}}$  through the calculation of residual enthalpies of the two phases.

Thus, the central question that drives this study is: Which cubic equation of state—Soave-Redlich-Kwong (SRK) or Peng-Robinson (PR)—offers more accurate predictions of vapor-liquid equilibrium properties for ethylene across a relevant temperature range?

To answer this, we analyze and compare the EOS predictions against experimental data obtained from the NIST database. The reliability of each model is evaluated through graphical comparisons and statistical tools such as the Root Mean Square Error (RMSE). The objective is to identify the most suitable EOS for thermodynamic modeling of ethylene under different process conditions.

This study is divided into two main chapters: Chapter I focuses on the theoretical and conceptual background necessary for understanding vapor-liquid equilibrium (VLE). It presents fundamental thermodynamic principles, explores the phase behavior of pure substances, and introduces key concepts such as fugacity, compressibility, and enthalpy. The chapter also explains the development and mathematical formulation of the Soave-Redlich-Kwong (SRK) and Peng-Robinson (PR) equations of state, highlighting their applicability to real fluids. Chapter II applies these models to the case of ethylene, analyzing their ability to predict important thermodynamic properties such as saturation pressure, compressibility factors, molar volumes, and enthalpy of vaporization. The performance of each EOS is evaluated through graphical comparisons and quantitative error metrics using experimental data from the NIST database.

Finally, the study concludes with a general conclusion summarizing the findings and offering guidance on the most suitable EOS model based on the trade-off between simplicity and predictive accuracy for industrial applications, providing insights that can assist engineers and researchers in accurate process simulation and design.

# ***CHAPTER I***

*PVT Behavior for VLE for pure fluid and the importance of equation of state.*

## I.1. Introduction

Equilibrium is one of the fundamental tools available to chemical and environmental engineers. It holds equal importance to the others and is essential in a wide range of engineering applications. The various thermodynamic phases of a pure substance can be graphically represented in a pressure–temperature diagram, commonly referred to as a PT phase diagram. In this diagram, each phase occupies a distinct region. The coexistence of two phases such as solid–liquid or liquid–vapor—is shown as a line, indicating that for a given pressure, the transition between these two phases occurs at a specific temperature rather than across a temperature range.

Where two coexistence lines intersect, a triple point is formed—this is the unique condition at which three phases can exist in equilibrium simultaneously. Meanwhile, the liquid–vapor coexistence line ends at the critical point, beyond which the liquid and vapor phases become indistinguishable.

Classical thermodynamics equips us with powerful tools to analyze and interpret experimental data related to such phase behavior. However, it offers limited capability in predicting thermodynamic properties from first principles alone. A key principle in thermodynamic analysis is that nature tends to minimize Gibbs free energy. At equilibrium, any infinitesimal change in the system results in no change in Gibbs energy, indicating that the system is at its most stable configuration under the given constraints.

While the determination and prediction of vapor–liquid equilibrium (VLE) are the central objectives of this study, it is important to first to revisit some foundational thermodynamic principles. These principles provide the necessary background for the analyses and discussions that follow. Therefore, the aim of this chapter is to present an overview of thermodynamics as Thermodynamic concepts that have been applied in this work are discussed in this chapter. Explanation of phase and chemical equilibria, activity coefficients, fugacity and fugacity coefficients calculation using the equation of state and the relations between them are presented.

## I.2. Phase Equilibrium in a pure substance.

Consider as a system 1 kg of water contained in the piston/cylinder arrangement shown in Fig. I.1.a. Suppose that the piston and weight maintain a pressure of 0.1 MPa in the cylinder and that the initial temperature is 20°C. As heat is transferred to the water, the temperature increases appreciably, the specific volume increases slightly, and the pressure remains constant. When the temperature reaches 99.6°C, additional heat transfer results in a change of phase, as indicated in Fig. I.1.b. That is, some of the liquid becomes vapor, and during this process both the temperature and pressure remain constant, but the specific volume increases considerably. When the last drop of liquid has vaporized, further transfer of heat results in an increase in both the temperature and specific volume of the vapor, as shown in Fig. I.1.c.

When a substance exists as part liquid and part vapor at the saturation temperature, its vapor fraction is defined as the ratio of the mass of vapor to the total mass. This, in Fig. I.1.b, if the mass of the vapor is 0.2 kg and the mass of the liquid is 0.8 kg, the vapor fraction is 0.2 or 20%. The quality may be considered an intensive property and has the symbol  $x$ . Vapor fraction has meaning only when the substance is in a saturated state, that is, at saturation pressure and temperature.

If a substance exists as vapor at the saturation temperature, it is called saturated vapor. (Sometimes the term dry saturated vapor is used to emphasize that the Vapor fraction is 100%.) When the vapor is at a temperature greater than the saturation temperature, it is said to exist as superheated vapor. The pressure and temperature of superheated vapor are independent properties, since the temperature may increase while the pressure remains constant. Actually, the substances we call gases are highly superheated vapors. [1]

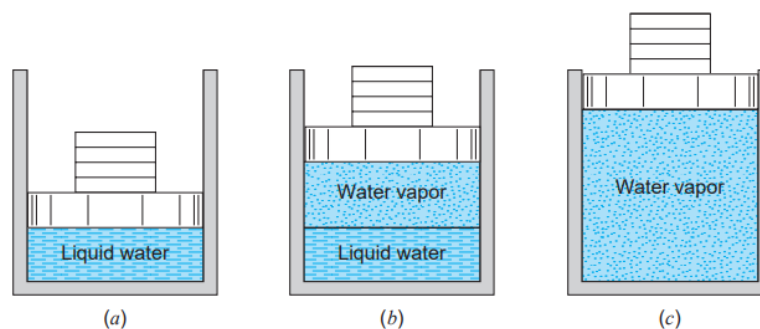


**Figure I-1:**Constant-pressure change from liquid to vapor phase for a pure substance

### I.3. P-V-T Behavior of Real Compounds.

To illustrate the interrelationships of physical properties of compounds, we consider the most commonly observed states of matter. Figure I.2 displays how the state of matter of a pure compound relates to pressure and temperature. As temperature increases at a constant pressure (e.g.,  $P_1$  in the diagram), the compound undergoes the familiar transition from solid to liquid to vapor. At lower pressures (e.g.,  $P_2$ ), no liquid phase occurs. Instead, at a certain temperature, the solid converts directly into gas, which is a process called sublimation. This is observed when dry ice (which is solid  $\text{CO}_2$ ) sublimates at ambient conditions.

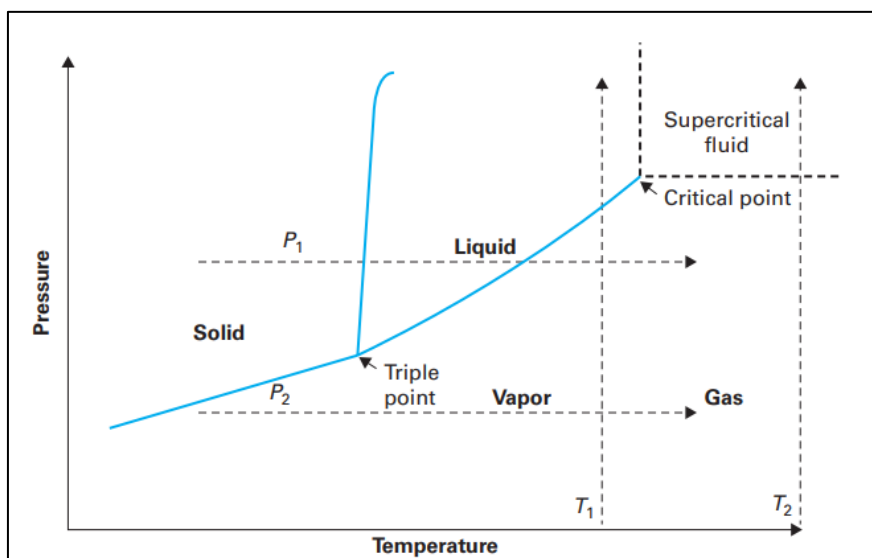


**Figure I-2:** Typical phase transition diagram for pure compounds.

The triple point temperatures and pressures for different compounds vary tremendously, for each individual compound, however, the triple point is unique. Consequently, the triple point is useful for providing repeatable temperatures for calibrations, the triple point of water is used as a reference point in defining the Kelvin temperature scale.

Figure I-3 shows the phase diagram of carbon dioxide ( $\text{CO}_2$ ). The triple point occurs at a temperature of  $56.57^\circ\text{C}$  (216.58 K) and at the pressure of 0.518 MPa (5.11 atm). As the pressure of the triple point is greater than 1 atm, the carbon dioxide does not exist in the liquid state at a pressure of 1 atm. At this pressure, the solid carbon dioxide passes directly to the gaseous state at a temperature of  $78.4^\circ\text{C}$  (194.7 K), a phenomenon known as sublimation. However, it is possible to obtain liquid carbon dioxide, for example, at the temperature of  $20^\circ\text{C}$ , increasing the pressure to 5.73 MPa (56.5 atm). The critical point of  $\text{CO}_2$  occurs at the temperature of  $30.99^\circ\text{C}$  (304.14 K) and at the pressure of 7.375 MPa (72.79 atm).

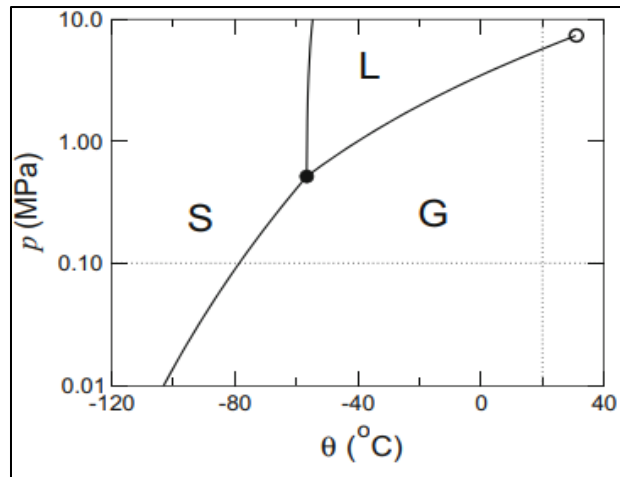


**Figure I-3:**Phase diagram of carbon monoxide (CO<sub>2</sub>) showing the gas (G), the liquid (L) and solid (S) phases.

- The horizontal dotted line indicates the pressure of 1 atm and the vertical dotted line, the temperature of 20 °C. The triple point is represented by a full circle and the critical point by an empty circle. [2]

#### I.4. PV Graph.

Beyond the question of which phase will be present at a particular temperature and pressure, the physical properties of a phase are also dependent upon temperature and pressure. The  $PV$  graph is the projection on the  $PV$  plane and is shown in Figure I-4. The characteristic feature of this graph is the vapor-liquid region, represented by a bell-shaped curve that consists of two branches, saturated liquid (to the left) and saturated vapor (to the right). The two branches meet at the top and this point defines the *critical point* of the fluid. Temperature is indicated by contours of constant temperature (isotherms). These are lines with the general direction from the upper left corner to the lower right. The isotherm that passes through the critical point corresponds to the critical temperature ( $T_c$ ). [3]

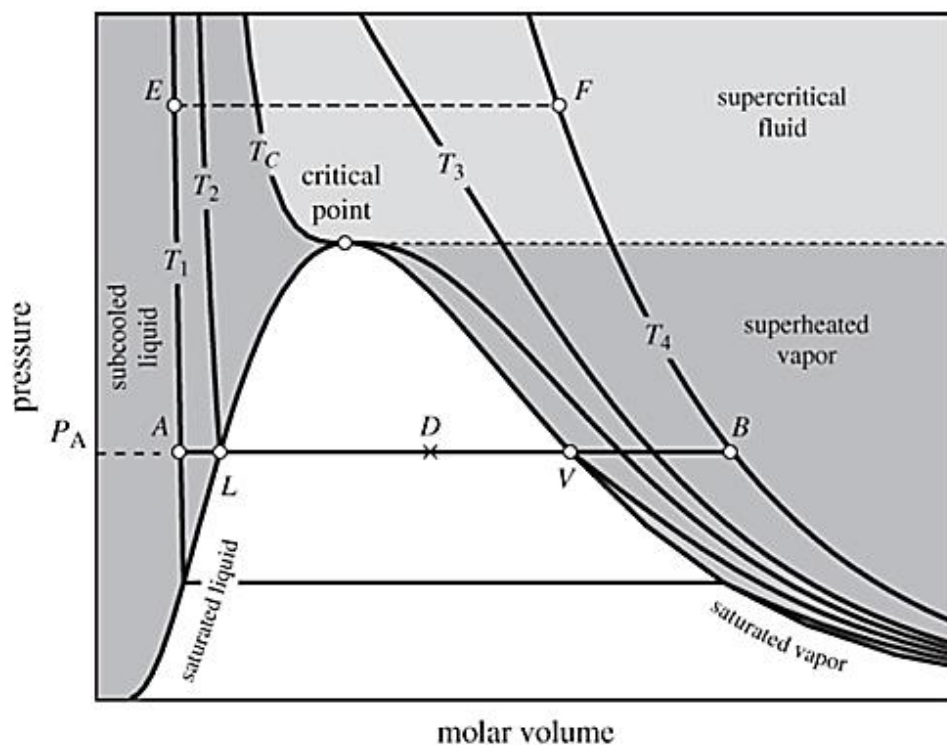


**Figure I-4:** The PV graph of pure fluid (the solid phase is not shown).

The critical point is an important state and its pressure and temperature have been tabulated for a large number of pure substances. In approaching the critical point from below, the distance between points  $L$  and  $V$  decreases, indicating that the molar volume of the saturated liquid and saturated vapor come closer together. At the critical point the two saturated phases coincide: vapor and liquid become indistinguishable and the phase boundary ceases to exist. The region of the phase diagram above  $P_c$  and  $T_c$  is referred to as supercritical fluid. No isotherms or isobars in this region intersect the vapor-liquid boundary. If point  $E$  is heated isobarically to final state  $F$ , one will observe a continuous transition from a dense, liquid-like state, to a dilute, gas-like state. In the supercritical region the notions of “liquid” and “vapor” are not helpful. These terms are meaningful when both phases can exist simultaneously and can be identified as distinct from each other. The term *supercritical fluid* avoids these ambiguities.

Properties near the critical point are quite different compared to states at lower temperatures and pressures. As the difference between vapor and liquid becomes less clear near the critical point, the liquid becomes substantially more compressible than typical liquids. This is indicated on the  $PV$  graph by the gentle slope of the isotherm as it approaches the critical point. Isotherms below but near the critical temperature (not shown in Figure I-4) show similar behavior. The usual approximation that treats liquids as incompressible is acceptable only at temperatures well below the critical. In the supercritical region, the behavior of a fluid is

somewhere between that of a liquid and a gas. The gentle slope of the isotherms indicates that the fluid is quite compressible, even at high (liquid-like) densities (low molar volumes). Other properties, in particular, the solubility of various nonvolatile solutes, are often found to be quite enhanced compared to the subcritical region. [3]

## I.5. Equilibrium Conditions at Constant T & P

In many practical situations we are dealing, not with isolated systems, but with systems that interact in various ways with their surroundings. An important case is a closed system that interacts with a bath at temperature  $T$  under constant pressure  $P$ . To study the equilibrium conditions for such a system, we apply the second law to the system and its surroundings:

$$\Delta S - \frac{Q}{T} = S_{gen} \quad \text{I-1}$$

Using  $Q = \Delta H$  (recall that the process occurs under constant pressure), this becomes

$$T\Delta S - \Delta H = TS_{gen} \quad \text{I-2}$$

We now introduce a new thermodynamic property, the *Gibbs free energy*,  $G$ , which we define as follows:

$$G = H - TS \quad \text{I-3}$$

For an isothermal process, such as the one considered here, the change in the Gibbs free energy is:

$$\Delta G = \Delta H - T\Delta S \quad (T = cst) \quad \text{I-4}$$

Combining these results, we obtain:

$$\Delta G = -TS_{gen} \leq 0 \quad \text{I-5}$$

This result states that during the process the Gibbs free energy decreases ( $\Delta G$  is negative) until equilibrium is reached, at which point  $G$  does not change any more ( $\Delta G$  is zero). In other words, the Gibbs free energy at equilibrium is at a minimum. Mathematically, [3]

$$(\Delta G \leq 0)_{T,P,n} \quad \text{I-6}$$

At equilibrium natural systems are, in effect, at the bottom of a Gibbs energy basin, in which for any infinitesimal change in any direction the change in Gibbs energy is zero, and for any finite change the Gibbs energy increases. All-natural systems try to lower their Gibbs energy. For any differential equilibrium change, chemical, physical or both, at constant T & P,

$$dG_{sys} = 0 \quad \text{I-7 [4]}$$

When a pure system can exist in more than one phases, as when the equation of state has multiple roots, the stable phase is identified as the one with the lowest Gibbs free energy. In this case, both phases are at the same pressure and temperature, but each has its own value of the Gibbs free energy. The stable phase is the one with the lower Gibbs free energy.

The thermodynamic behavior of pure substances can be effectively modeled using equations of state (EOS). These mathematical formulations establish fundamental relationships between pressure (P), volume (V), and temperature (T) for a given system. Several important EOS formulations have been developed over time, ranging from the simple Ideal Gas Law to more sophisticated equations such as the Redlich-Kwong (RK), and Peng-Robinson (PR) equations. Each of these equations offers varying levels of accuracy and complexity in describing real fluid behavior.

A detailed examination of these equations and their applications will be presented in the following section.

## **I.6.PVT Behavior of low & moderate density gases.**

All gases behave ideally when the pressure approaches zero. The pressure volume relation for an ideal gas is,

$$PV = nRT \quad \text{I-8}$$

where  $v$  is the molar volume,  $P$  is (absolute) pressure,  $T$  is (absolute) temperature, and  $R$  is the universal gas constant (Table A. in Appendix). Hence one mole of any ideal gas occupies the same volume at a given pressure and temperature.

In engineering applications, gases at the standard conditions can be treated as ideal. The occupied volume of one mole of gas at various standard conditions. [5]

Note that for the ideal gas equation both the pressure  $P$  and the temperature  $T$  must be expressed in absolute quantities.

Consider for example the P-V diagram as shown below:

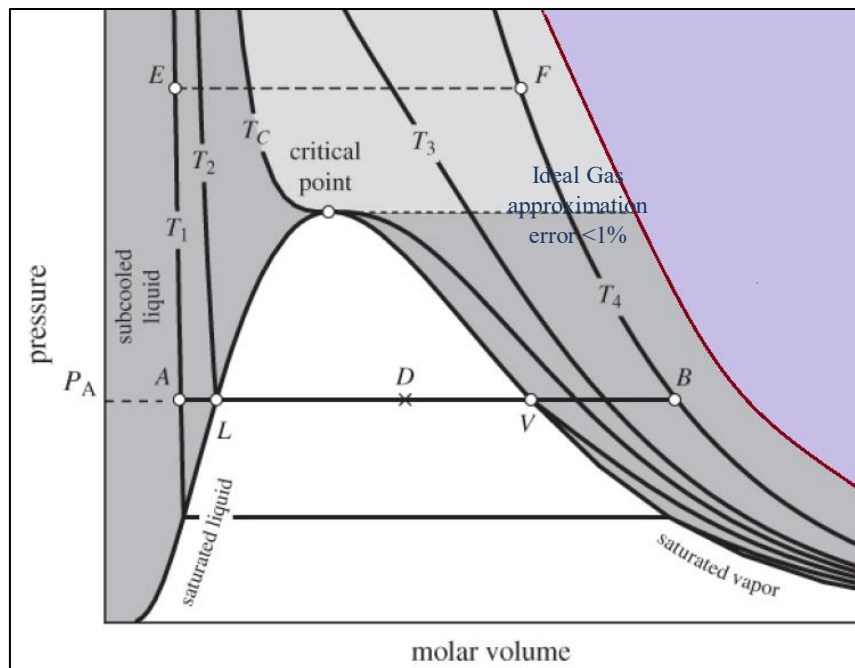


**Figure I-5:** The PV graph of pure fluid with showing the isotherm of the ideal gas.

The shaded zone in the diagram indicates the region that can be represented by the Ideal Gas equation to an error of less than 1%.

- Continuing on our discussion of pure substances, we find that for a pure substance in the superheated region at specific volumes much higher than the critical point, the  $P$ - $v$ - $T$  relation can be conveniently expressed very accurately by the Ideal Gas Equation of State (I.8) [6]
- An ideal gas is an imaginary substance that obeys the relation  $Pv = RT$ . It has been experimentally observed that the ideal-gas relation given closely approximates the  $P$ - $v$ - $T$  behavior of real gases at low densities. At low pressures and high temperatures, the density of a gas decreases, and the gas behaves as an ideal gas under these conditions.

So, what about the other conditions? What constitutes low pressure and high temperature is explained next. [7]

## I.7. Compressibility Factor.

We noticed in the above  $P$ - $v$  diagram that the gasses can deviate significantly from the ideal gas equation of state in regions nearby the critical point and there have been many equations of state recommended for use to account for this non-ideal behavior. However, this non-ideal behavior can be accounted for by a correction factor called the Compressibility Factor  $Z$ . [8]

Due to intermolecular forces real gases do not behave ideally, particularly at elevated pressures. Eq. (I-6) is extended to real systems by including a compressibility factor,  $Z$ , as,

$$PV = ZRT \quad \text{I-9}$$

The compressibility factor can be determined from various theoretical-empirical equations of state, or determined from a generalized chart for gases (chart A.I in Appendix B). Note that the compressibility factor depends only on the ratio of temperature to critical temperature (absolute), the reduced temperature,  $T_r$ , and the ratio of pressure to critical pressure, the reduced pressure,  $P_r$ .

The above approach is based on a very important concept, known as the corresponding states principle, which states that substances behave similarly when they are at the same relative proximity to their critical points. This implies that all substances behave similarly at their critical points, hence, should have equal critical compressibility factor,  $Z_c$ ,

$$Z_c = \frac{P_c V_c}{R T_c} \quad \text{I-10}$$

The real value of critical compressibility factor, however, is not the same for all compounds (Table A. 1 in Appendix A). The compressibility chart, however, provides reliable estimates particularly for supercritical gases and at low pressure conditions. Charts relating the compressibility factor to the reduced pressure and temperature, similar to (chart A.I in Appendix B). [5]

- By including the compressibility factor in equations of state (EoS), such as van der Waals or Peng-Robinson equations, engineers and scientists are able to more accurately predict the behavior of gases in industrial and scientific applications.
- We will see in the next point the different equations of states

## **I.8. Cubic Equations of State.**

Formally, an equation of state is a relationship among temperature, pressure, and molar volume, such that if any two are known, the third can be calculated. Thus, the ideal gas law is an equation of state that has practical value at low pressures. However, at elevated pressures, real gases exhibit substantial departure from ideal gas behavior. Many more complex equations of state have been proposed to quantify  $P$ ,  $V$ , and  $T$  at a broader range of conditions.

For engineering calculations, it is important to have equations of state that are accurate over a wide range of pressures and temperatures. As we mention before the ideal gas law is very

simple to use, but its validity is restricted to gases at low pressures. The truncated virial equation is applicable over a somewhat wider range of pressures, but only for gases. If the pressure is high or the phase liquid, neither of these equations can be used. Numerous empirical equations of state have appeared in the literature to overcome these difficulties. Such equations usually have some theoretical basis, but the primary consideration is sufficient accuracy for engineering applications. It is typical for these equations to contain parameters that are fine-tuned to improve accuracy. No single mathematical equation of state can describe all fluids. Nonetheless, it is convenient in having one equation whose mathematical form is the same for many fluids but with parameters that are specific to a particular fluid. Among the most important engineering equations of state is the family of cubic equations, which can be viewed as variants of the van der Waals equation of state.

### **I.8.1. Van der Waals Equation.**

The Van der Waals equation of state, proposed in 1873 (Rowlinson,1988), was the first equation capable of representing vapor-liquid coexistence.

$$Z = \frac{v}{v-b} - \frac{a}{RTv} \quad \text{I-11} \quad ; \quad a = \frac{27R^2T_{cr}^2}{64P_{cr}} \quad \text{I-12} \quad ; \quad b = \frac{RT_{cr}}{8P_{cr}} \quad \text{I-13}$$

where  $Z$  is the compressibility factor  $Z = pV / RT$ ;  $T$  is temperature,  $V$  is volume,  $p$  is the pressure, and  $R$  is the molar universal gas constant. The parameter  $a$  is a measure of the attractive forces between the molecules, and the parameter  $b$  is the volume occupied by the molecules. The  $b$  parameters can be obtained from the critical properties of the fluid. [9]

While qualitative, these explanations of “ $a$ ” and “ $b$ ” allow us to rationalize the van der Waals equation compared to the ideal gas law. [9]

- The van der Waals equation is a cubic EOS—it is first degree in  $T$  and  $P$  but third degree in  $V$ . Consequently, for a given  $T$  and  $P$ , there are three solutions for  $V$  (although in some circumstances two solutions are imaginary). Although the van der Waals equation is no longer in common use, we will see next that there are equations of state in common use that are more complex variants of the van der Waals equation.
- The Van der Waals equation was one of the earliest attempts to correct the ideal gas law by accounting for intermolecular interactions and the finite volume of gas molecules. However, it remains inaccurate for many industrial applications, especially at high pressures and temperatures near the critical point.

- This is why more precise equations were developed, such as the PR (Peng-Robinson) and SRK (Soave-Redlich-Kwong) equations.

### I.8.2 Soave Redlich Kwong Equation.

In 1949 (Redlich and Kwong, 1949), the Redlich–Kwong (RK) equation of state was considered a significant improvement over other equations of the time. It is still of interest primarily due to its relatively simple form. While superior to the van der Waals equation of state, it performs poorly with respect to the liquid phase and thus cannot be used for accurately calculating vapor-liquid equilibria. However, it can be used in conjunction with separate liquid-phase correlations for this purpose. The Redlich–Kwong equation was mainly coined to predict the properties of small, non-polar molecules in the vapor phase, which it generally does well. However, it had been subject to various attempts to refine and improve it. In 1972, Soave (1972) replaced the  $(1/\sqrt{T})$  term of the Redlich–Kwong equation with a function  $\alpha(T,\omega)$  involving the temperature and the acentric factor (the resulting equation is also known as the Soave–Redlich–Kwong equation, SRK). The  $\alpha$  function was devised to fit the vapor pressure data of hydrocarbons and the equation does fairly well for such materials. [10]

The Soave-Redlich-Kwong equation of state is given by

$$Z = \frac{v}{v-b} - \frac{a(T)}{RT(v+b)} \quad \text{I-14}$$

Where, a and b are parameters specific to the fluid and are given in terms of the critical pressure, critical temperature, and acentric factor:

$$a(T) = 0.42748 \frac{R^2 T_{cr}^2}{P_{cr}} \alpha(T) \quad \text{I-15}$$

$$b = 0.08664 \frac{RT_{cr}}{P_{cr}} \quad \text{I-16}$$

$$\alpha(T) = (1 + (0.48 + 1.574\omega - 0.176\omega^2) \left(1 - \sqrt{\frac{T}{T_{cr}}}\right))^2 \quad \text{I-17}$$

( $\omega$ =acentric factor)

$$Z^3 - Z^2 + (A - B - B^2)Z - AB = 0 \quad \text{I-18}$$

$$\text{Where, } A = \frac{aP}{(RT)^2} \quad \text{I-19}$$

$$B = \frac{bP}{RT} \quad \text{I-20}$$

### I.8.3. Peng Robinson Equation.

The Peng-Robinson (PR) equation of state slightly improves the prediction of liquid volumes and predicts a critical compressibility factor of  $Z_c = 0.307$ . Peng and Robinson (1976) the original article gave examples of the use of their equation for predicting the vapor pressure and volumetric behavior of single-component systems, and the phase behavior and volumetric behavior of the binary, ternary, and multicomponent system and concluded that Eq. (I-21) can be used to accurately predict the vapor pressures of pure substances and equilibrium ratios of mixtures. The Peng-Robinson equation performed as well as or better than the Soave Redlich-Kwong equation.

Han et al. (1988) reported that the Peng-Robinson equation was superior for predicting vapor-liquid equilibrium in hydrogen and nitrogen containing mixtures, this article compares seven equations of state, including Peng–Robinson, with experimental data for mixtures of non-polar and slightly polar substances.

The Peng Robinson equation of state is given by

$$Z^3 + (B - 1)Z^2 + Z(A - 3B^2 - 2B) - AB + B^3 + B^2 = 0 \quad \text{I-21}$$

Where,

$$a(T) = 0.45724 \frac{R^2 T_{cr}^2}{P_{cr}} \alpha(T) \quad \text{I-22}$$

$$\alpha(T) = \left( 1 + (0.37464 + 1.54226\omega - 0.26992\omega^2) \left( 1 - \sqrt{\frac{T}{T_{cr}}} \right) \right)^2 \quad \text{I-23}$$

$$b = 0.0778RT_{cr}/P_{cr} \quad \text{I-24}$$

( $\omega$  : acentric factor)

The Peng-Robinson and Soave-Redlich-Kwong equations are used widely in industry. The advantages of these equations are that they can accurately and easily represent the relation among temperature, pressure, and phase compositions in binary and multicomponent systems. They only require the critical properties and acentric factor for the generalized parameters. [9]

## I.9.Saturation Pressure Determination

At given temperature we must determine the saturation pressure that achieves the equilibrium condition. So, let's see the process. We want to determine the precise conditions that define the saturation point. For this we turn to the Gibbs free energy and in particular to eq. (I-5), which

states that the equilibrium state of a system at constant T, P, and n, is such that the Gibbs free energy is at a minimum.

We imagine the following experiment: a fixed number of moles of a fluid is placed in a closed system at such pressure and temperature as to form two phases. The pressure and temperature are then maintained constant (for example, using a movable piston and a heat bath). Suppose that we take a small number of  $\delta n$  moles and transfer them from the liquid to the vapor. The new state is also an equilibrium two-phase system and since the Gibbs free energy is at a minimum, this transfer should cause no change in the total Gibbs free energy of the system. However, the Gibbs free energy of the individual phases changes because G is an extensive property and depends on the number of moles. Specifically, the Gibbs free energy of the liquid changes by  $-G_L \delta n$  and that of the vapor by  $+G_V \delta n$ . For the total Gibbs free energy to remain constant regardless of the number of moles that are transferred, we must have  $G_L = G_V$  [3].

- Starting from the same principle presented above, several methods of Saturation Pressure determination have been developed, next some examples are presented.
- In our work, we will use the 3<sup>rd</sup> method (using EOS), but in order to get some fundamental insights, we will start by giving some details about the fundamental method, using the Clapeyron, & the Clausius Clapeyron formulations, then, the well-known Antoine's method.

### **I.9.1. Methods of calculation the Saturation Pressure**

For calculating the saturation pressure of a pure substance and understanding vapor-liquid equilibrium (VLE), several methods are commonly used depending on the context whether for pure substances or mixtures in equilibrium.

#### **I.9.1. Using Antoine equation**

A popular one is the Antoine equation. it was developed based on the Clapeyron equation. It has been widely used to estimate the vapor pressure over limited temperature ranges. The proposed model is shown below:

$$\ln P_{sat}(T) = A - \frac{B}{T + C} \quad \text{I-25}$$

with:

$$A = \ln P_{sat}(T_0) + \frac{\Delta H_{vap}}{R T_0} \quad \text{I-26}; \quad B = \frac{\Delta H_{vap}}{R} \quad \text{I-27} \quad \text{and} \quad C = 0$$

where A, B, and C, are empirical constants fitted to experimental data.

The basic equation is stated in a corresponding state type formula with the reduced pressure and temperatures as variables and the Acentric Factor ( $\omega$ ) as parameter. It reads as follows:

$$\ln(Pr) = 5.3727 \times (1 + \omega) \times \left(1 - \frac{1}{Tr}\right) \text{I-28}$$

$$Pr = \frac{P_{sat}}{P_c} \text{I-29} \quad ; \quad Tr = \frac{T_{sat}}{T_c} \text{I-30}$$

where  $Pr$  and  $Tr$ , are the reduced vapor pressure and temperature and  $\omega$  is the acentric factor, is a correct and recognized generalized vapor pressure correlation used in thermodynamics and engineering.

This equation is valid for the following reduced temperature range:  $0.70 = < Tr = < 1.0$ .

The actual (saturated) vapor pressure as function of the absolute temperature can be expressed as:

$$P = P_c * \text{Exp} ( 5.3727 * (1 + W) * (1 - Tc / T) ) \quad \text{I-31}$$

The advantage of the equations is they are simple, versatile and are applicable to a very wide range of substances. The ready availability of the Acentric Factor in many thermo-physical databases adds to its wide-ranging usefulness. The downside is that these equations, by definition, have a limited validity range covering only the ‘upper’ part of the entire two-phases vapor liquid region the reduced temperature range of  $Tr = 0.7$  to  $1.0$ . [8]

- Final method is the Equation of State which is a mathematical model that relates pressure, temperature, and volume (or molar volume/density) of a substance. It's used to predict thermodynamic properties (like vapor pressure, compressibility, enthalpy, fugacity, etc.) especially for real gases and fluids.

### **I.9.3. Using Equation of state EOS**

The equation of state is one of the methods which we can determine the  $P_{sat}$  for pure substance. If we took the SRK EOS as an example; and using equations (I-15 to I-20).

The calculation is started by the parametrization step, on which the parameters such as  $b$ ,  $A$ ,  $B$  and  $\alpha$ , are calculated using the critical point coordinates of the substance. After that, the model is ready to use.

In order to get the  $P_{sat}$  value, Trial & Error method is used, and for each iteration we perform a sequence of steps, as described in below:

- At the desired  $T < T_c$ , we choose an initial guess of Saturation pressure:
- Using  $T$  &  $P_{sat}$  values, the Compressibility factor 3 roots can be obtained by solving the Cubic SRK EOS ( $Z_{min} = Z_{liq}$  &  $Z_{max} = Z_{vap}$ ), using Newton's method;
- Using  $Z_l$  &  $Z_v$ , fugacity coefficients ( $\phi_v, \phi_l$ ) for each phase can be deduced using eq (I-32)

$$\ln \phi = Z - 1 - \log(Z - B) - (A/B) * \log(1 + B/Z) \quad \text{I-32}$$

$$\phi = \exp(\ln \phi)$$

- Convergence Test: Check if Fugacity coefficient ratio = 1, >1 or < 1;
- Based on the ratio, New  $P_{sat}$  is chosen, and we repeat same steps, until desired precision is obtained
- We compute the fugacity coefficients for both vapor and liquid using these following equations:

$$\ln \phi_{vap} = Z_{vap} - 1 - \log(Z_{vap} - B) - (A/B) * \log(1 + B/Z_{vap}) \quad \text{I-33}$$

$$\ln \phi_{liq} = Z_{liq} - 1 - \log(Z_{liq} - B) - (A/B) * \log(1 + B/Z_{liq}) \quad \text{I-34}$$

- To solve these equations, we need a numerical function to compute the compressibility factor for a real gas using SRK EOS)
- The SRK EOS leads to a cubic equation in  $Z$ , which accounts for non-ideal gas behavior through two dimensionless parameters:  $A$ , representing attractive molecular forces, and  $B$ , representing repulsive interactions due to finite molecular volume. The function uses the Newton-Raphson method to solve this cubic equation iteratively, with different initial guesses based on the desired phase (vapor or liquid). The parameter  $B$  plays a key role not only in shaping the cubic equation but also in ensuring physical realism by constraining  $Z$  to be greater than  $B$ , since  $Z$  is linked to molar volume and must remain above the excluded volume defined by the repulsion parameter. This approach ensures accurate and stable determination of thermodynamic properties for real gases.
- The above steps are presented next with more details.

➤ **Step 1: Define the cubic function  $f(Z)$**

The cubic EOS can be written in the standard form:

$$f(Z) = Z^3 + a_2Z^2 + a_1Z + a_0$$

Where,

$$a_2 = -1;$$

$$a_1 = A - B - B^2;$$

$$a_0 = -AB$$

$$f(Z) = Z^3 - Z^2 + (A - B - B^2)Z - AB$$

➤ **Step 2: Choose an initial guess  $Z_0$ :**

- For vapor phase: use  $Z_0 \approx 1$ . (Since vapor tends to have higher  $Z$ ).
- For liquid phase: use  $Z_0 \approx 1.5 \times B$  (closer to real liquid behavior).

➤ **Step 4: Perform Newton-Raphson Iteration:**

- Applying the Newton-Raphson update formula and check for convergence
- Next, Ensure physical constraints

➤ **Step 5: Add safety checks during iteration:**

- If the derivative  $f'(Z)$  is too small (close to zero), slightly perturb  $Z$  to avoid division by zero.
- If  $Z \leq BZ$ , adjust  $Z$  to a value slightly above  $B$ , since compressibility factor must be greater than for a real fluid.
- For liquid phase, if  $Z$  becomes too large (e.g.,  $Z > 1$ ), re-adjust to a more liquid-like value.

➤ **Step 6: Check phase-specific and physical validity:**

After convergence:

- For vapor phase, ensure  $Z > B$
- For liquid phase, ensure  $Z \lesssim 1$

- In all cases,  $Z$  must be positive.
  - After saturation pressure is obtained, its value can be used to calculate a very important property, which is the Vaporization Enthalpy. The calculation Procedure of this property is presented in details in the next section.

## I.10. Vaporization Enthalpy Calculation Procedure

The enthalpy of vaporization is the energy required to convert a substance from liquid to vapor at constant temperature and pressure. It is essential in phase change processes. This section presents the main steps used to calculate it using thermodynamic methods.

1. **Calculate the parameters:**  $T_r$ ,  $\alpha(T)$ ,  $a$ ,  $b$ : The SRK EOS and PR are relying on two fundamental parameters, denoted  $a$  and  $b$ , which represent the attractive and repulsive interactions between molecules, respectively. These parameters are derived from the critical properties of the substance: the critical temperature  $T_c$ , critical pressure  $P_c$ , and acentric factor  $\omega$ .

The expressions used to calculate these parameters are mentioned in eq (I-16) , (I-17), for SRK and eqs (I-23), (I-24) for PR

2. **Calculation of the Dimensionless Coefficients A and B:**

Once the SRK and PR parameters  $a$ ,  $b$ , and the temperature correction factor  $\alpha(T)$  have been determined, the next step is to calculate the dimensionless coefficients  $A$  and  $B$ . These coefficients simplify the cubic formulation of the SRK and PR equation of state and facilitate the determination of the compressibility factor  $Z$

3. **Determination of Compressibility Factors ( $Z$ ):**

Once the cubic equation is solved using either SRK or PR, the compressibility factors  $Z_l$  and  $Z_v$  are obtained for the liquid and vapor phases, respectively. These values are fundamental for the next step, where they are used to calculate the residual enthalpies of each phase. The accuracy of the enthalpy of vaporization depends significantly on the correct identification and use of these roots.

- ✚ The equation for the compressibility factor for the SRK and PR is respectively defined in eq (I-18), (I-21)

- 4. Calculation of residual enthalpies ( $H^R$ ) for vapor and liquid:** The residual enthalpy is therefore calculated separately for the vapor phase and the liquid phase, using the corresponding  $Z$  values obtained in the previous step by solving the cubic equation.

✚ Soave-Redlich-Kwong (SRK):

$$H^R = RT(Z - 1) + \frac{T \left( \frac{da}{dT} \right) - a}{b} \ln \frac{Z + B}{Z} \quad \text{I-35}$$

✚ Peng-Robinson (PR):

$$H_R = RT(Z - 1) + \frac{T(da/dT) - a}{2\sqrt{2}b} \ln \frac{(1 + \sqrt{2})Z + B}{(1 - \sqrt{2})Z + B} \quad \text{I-36}$$

Where for both SRK and PR equations, the derivative  $da/dT$  is calculated using:

$$\frac{da}{dT} = -0.42748 \frac{R^2 T_c \left( 1 + \Omega(1 - \sqrt{T_r}) \right) \Omega}{\sqrt{T_r}} \quad \text{I-37}$$

$$\frac{da}{dT} = -0.45724 \frac{R^2 T_c \left( 1 + \Omega(1 - \sqrt{T_r}) \right) \Omega}{P_c \sqrt{T_r}} \quad \text{I-38}$$

$\Omega$  : is the acentric factor correlation specific to each equation of state. [3]

- 5. Calculation of Enthalpy of Vaporization:** Once the residual enthalpies of the two phases (liquid and vapor) have been obtained in the previous step, it is possible to determine the enthalpy of vaporization.

Using this equation:

$$\Delta H_{vap} = H_R^L - H_R^V \quad \text{I-39}$$

Next, and in order to be able to evaluate the performance of each EOS, deviation will be investigated using the Root Mean Squared Error calculation. [3]

## I.11. Root Mean Squared Error

The root mean square error RMSE is defined as the measure of the differences between values that are predicted by a model and values that are actually observed. Here,  $N$  is the number of observations

$$RMSE = \sqrt{\frac{\sum_{i=1}^N (\text{Predicted}_i - \text{Actual}_i)^2}{N}} \quad I-40$$

- *Predicted*: are predicted values.
- *Actual<sub>i</sub>*: are observed values
- $N$ : is the number of observations. [11]

# ***CHAPTER II***

*Interpretation and evaluation the results of  
calculation*

## **II.1. Introduction.**

Cubic equations of state (EoS), such as van der Waals, Redlich-Kwong, Soave-Redlich-Kwong (SRK), and Peng-Robinson (PR), are widely used in thermodynamics due to their simplicity, computational efficiency, and ability to model both liquid and vapor phases. These equations require only a few input parameters, such as critical properties and the acentric factor, making them practical for industrial applications. They accurately predict phase behavior, including vapor-liquid equilibrium (VLE) and critical points, and are commonly used in process simulation software for refining, petrochemicals, and natural gas processing.

This practical section of our project delves into the application and comparative analysis of two prominent cubic equations of state: the Soave-Redlich-Kwong (SRK) and the Peng-Robinson (PR) EOS. Both SRK and PR offer valuable tools for predicting thermodynamic properties and phase behavior in chemical engineering, with each exhibiting strengths and weaknesses depending on the system and conditions.

The present research seeks to evaluate the ability of two highly used cubic equations of state (Soave-Redlich-Kwong or SRK and Peng-Robinson or PR) to simulate the thermodynamic properties of pure compounds over a temperature domain. First, we will produce pressure-volume isotherms to compare graphically the predictions from both EOS to experimental levels. Afterwards, the prediction of saturation volumes of each model will be tested on quantitative measures such as percentage error to determine their accuracy. This visual and numerical analysis will assist in determining which equation of state gives the most reliable predictions in different thermodynamic conditions.

As an example, to pretend the behavior of pure compound we use the ethylene an Hydrocarb

Component a light hydrocarbon widely used in the petrochemical industry, particularly as a raw material in the production of polymers

## II.2. Experimental data of ethylene from NIST.

Behind our assessment of the EOS models is a framework consisting of credible experimentation data. This section will take a look into the PV data gathered for ethylene. We will use this data as a baseline to compare EOS predictions.

## II.3. Experimental PV diagram of ethylene from NIST.

In order to see the relationship between pressure (P) and volume (V) of ethylene, we'll plot pressure-volume (PV) diagrams. These diagrams will be based on valid experimental data obtained from the NIST. [12]

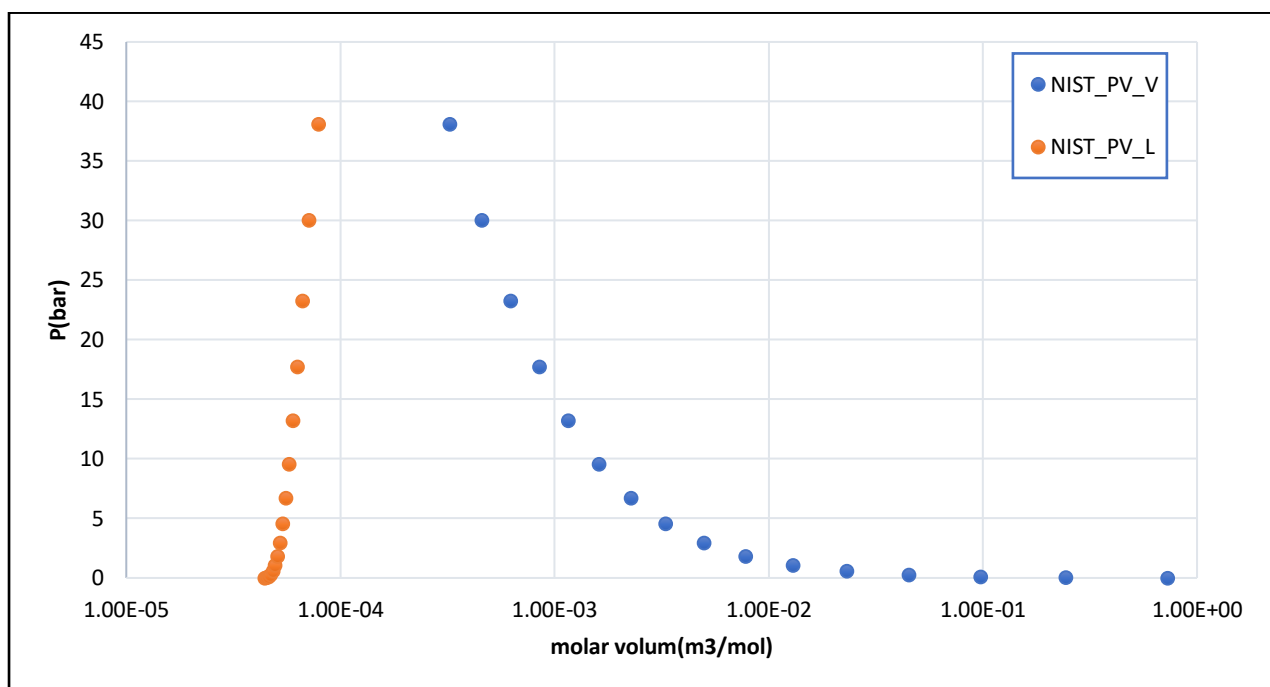


Figure II-1: Experimental PV diagram plotting for ethylene.

## II.4.SRK EOS Performances Evaluation

The Soave-Redlich-Kwong (SRK) equation of state enhances the accuracy of PVT modeling for real gases by introducing an attraction term correction based on the acentric factor. It is particularly effective for light hydrocarbons. Plotting SRK isotherms (pressure vs. molar volume at constant temperature) illustrates non-ideal behavior, phase transitions, and near critical phenomena. This approach is essential for analyzing thermodynamic equilibria in industrial process applications.

- Next, we will mention the calculation steps of the program code using MATLAB by taking the temperature,  $110 < T \text{ (K)} < 280$

### II.4.1. SRK EOS Parameterization Steps

- Using the characteristics of this EOS presented in Chapter1, the parametrization of this model was established using MATLAB, as presented in the FigII-2

```
R = 0.08314472; % bar.L/mol.K

% SRK parameters
Tr = T / Tc;
m = 0.480 + 1.574 * w - 0.176 * w^2;
alpha = (1 + m * (1 - sqrt(Tr)))^2;
a = 0.42748 * (R^2) * (Tc^2) / Pc * alpha;
b = 0.08664 * R * Tc / Pc;

% Dimensionless parameters
A = a * P / (R^2) / (T^2);
B = b * P / (R * T);
```

**Figure II-2:** Calculation of SRK parameters.

### II.4.2. Steps of calculation the saturation pressure.

- Using the process shown in the first chapter section (I.9).

#### 1. Initial Estimate.

- Fig. II-3 is one of methods mentioned in I-9, used it here to start with Psat initial estimate

```
% Initial estimate of Psat
Psat = Pc * exp(5.3727 * (1 - Tc / T));
```

**Figure II-3:** Initial estimate of Psat

Where: Pc = Critical pressure; Tc = Critical temperature; T = System temperature

#### 2. Iterative Calculation Process.

- For,  $120 < T < 270$  we calculate:

```
for T = 120:10:270

% Calculate saturation pressure and properties
[Psat, Zv, Zl, phiV, phiL] = calculate_saturation(T, Tc, Pc, w);

% Calculate residual enthalpies for both phases
Hr_v = calculate_residual_enthalpy_v(T, Psat, Tc, Pc, w, Zv);
Hr_l = calculate_residual_enthalpy_l(T, Psat, Tc, Pc, w, Zl);

% Store data for CSV
data = [data; T, Psat, phiV, phiL, Zv, Zl, Hr_v, Hr_l];

% Display results for each temperature
fprintf('% .2f\t\t%.4f\t\t%.6f\t%.6f\t%.6f\t%.6f\t%.6f\n', ...
        T, Psat, phiV, phiL, Zv, Zl, Hr_v, Hr_l);

end
```

**Figure II-4:** Iterative Calculation of the parameters

### 2.1.Setup Parameters.

- Set maximum iterations (max-Iter = 200)
- Define tolerance (tol = 1e-8)
- Set pressure increment (dP = 0.01)

```
% Iteration parameters
maxIter = 200;
tol = 1e-8;
dP = 0.01;
```

**Figure II-5:**Iteration parameters

### 2.2.Main Iteration Loop.

- For each iteration we calculate the fugacity coefficient of both the vapor and liquid phases if their differences are small enough, the loop is terminated if it doesn't recalculate with  $P=P_0+0.01$ .

```
for iter = 1:maxIter
    % Calculate fugacity coefficients
    [phiV, Zv] = fugacity_coeff(T, Psat, Tc, Pc, w, 'V');
    [phiL, Zl] = fugacity_coeff(T, Psat, Tc, Pc, w, 'L');

    err = abs(phiV - phiL);

    if err < tol
        break;
    end
```

**Figure II-6:**The main iteration of fugacity coefficient

#### a) Calculate error: $err = |\phi_V - \phi_L|$ :

This iterative process ensures vapor-liquid equilibrium where the fugacity of both phases is equal, indicating thermodynamic equilibrium at the calculated saturation pressure.

- Check Convergence:
- If  $err < tol$ , calculation is complete, if not, continue iteration.

#### b) Solve cubic equation.

- ✚ using the steps as shown in the theoretical section we calculate the cubic equation of the compressibility factor and determined the two real roots needed for the both phases.

```

function Z = solve_SRK_cubic(A, B, phase)
    % Convert SRK cubic equation to reduced form:  $x^3 + a_2x^2 + a_1x + a_0 = 0$ 
    % From:  $Z^3 - Z^2 + (A-B-B^2)Z - AB = 0$ 
    a2 = -1; % coefficient of  $Z^2$ 
    a1 = A - B - B^2; % coefficient of  $Z$ 
    a0 = -A*B; % constant term

    % Initial guess based on phase
    if strcmpi(phase, 'V')
        Z = 1.0; % Initial guess for vapor phase
    else
        Z = B * 1.5; % Initial guess for liquid phase (slightly above B)
    end

    % Newton-Raphson iteration parameters
    maxIter = 100;
    tol = 1e-8;

    for i = 1:maxIter
        % Calculate function value f(Z)
        f = Z^3 + a2*Z^2 + a1*Z + a0;

        % Calculate derivative f'(Z)
        df = 3*Z^2 + 2*a2*Z + a1;

        % Check for zero derivative
        if abs(df) < 1e-12
            Z = Z + 0.01; % Small perturbation
            continue;
        end

        % Newton-Raphson update
        Z_new = Z - f/df;

        % Check convergence
        if abs(Z_new - Z) < tol
            Z = Z_new;
            break;
        end

        Z = Z_new;

        % Ensure physical constraints
        if Z <= B
            Z = B * 1.1; % Keep Z above B for physical meaning
        end
    end

    % Phase-specific validation
    if strcmpi(phase, 'V') && Z < B
        Z = B * 1.1; % Vapor phase must have  $Z > B$ 
    elseif strcmpi(phase, 'L') && Z > 1.0
        % For liquid phase, if  $Z > 1$ , try a different approach
        Z = B * 1.2; % Reset to liquid-like value
    end

    % Final validation - ensure Z is physically meaningful
    if Z <= 0
        error('Invalid compressibility factor: Z must be positive');
    end
end

```

**Figure II-7:** Numerical Resolution of the SRK Cubic Equation

- ✚ The SRK EOS function is designed to compute the compressibility factor  $Z$  by solving the cubic equation derived from the (SRK) equation of state.
- ✚ Next, we will explain step by step this function

➤ **Step 1: Formulate the Cubic Equation**

The SRK equation of state is rewritten in the following cubic form:  $Z^3 + a_2 Z^2 + a_1 Z + a_0 = 0$

➤ **Step 2: Set Initial Guess Based on Phase**

- If the phase is **vapor**  $Z=1.0$
- If the phase is **liquid**  $Z=1.5*B$

➤ **Step 3: Start Newton-Raphson Iteration Loop**

The function enters a loop to iteratively solve for  $Z$  using the Newton-Raphson method.

At each iteration:

- The value of the function  $f(Z)$ .
- Its derivative  $f'(Z)$ .
- And we update  $Z$  using the formula:  $Z_{new} = Z - \frac{f'(Z)}{f(Z)}$
- Check for convergence:

If  $|Z_{new} - Z| < 10^{-8}$ , the solution is accepted and the loop ends.

- Update  $Z$ :
- If the derivative is too small, a small correction is added.
- If  $Z \leq B$ , the value is adjusted to  $Z=1.1*B$  to ensure physical validity.

➤ **Step 4: Phase-Based Final Adjustment**

- If vapor phase and  $Z < B$ , enforce  $Z=1.1*B$
- If liquid phase and  $Z > 1.0$ , reset  $Z=1.2*B$

➤ **Step 5: Final Validation**

- If  $Z \leq 0$ , the function throws an error: compressibility factor must be positive

- Otherwise, the final value of Z is returned.

**c) Calculate Fugacity Coefficients**

After convergence, fugacity coefficients can be easily calculated using :

```
% Calculate fugacity coefficient
lnPhi = Z - 1 - log(Z - B) - (A / B) * log(1 + B / Z);
phi = exp(lnPhi);
```

**Figure II-8:**Fugacity coefficients calculation.

- Compute vapor phase fugacity (phiV)
- Compute liquid phase fugacity (phiL)

**d) Newton Method Update:**

- Calculate numerical derivative:

```
% Numerical derivative for Newton method
[phiV_plus, ~] = fugacity_coeff(T, Psat + dP, Tc, Pc, w, 'V');
[phiL_plus, ~] = fugacity_coeff(T, Psat + dP, Tc, Pc, w, 'L');
deriv = ((phiV_plus - phiL_plus) - (phiV - phiL)) / dP;
```

**Figure II-9:**Numerical derivative for the fugacities

- **Update Pressure:**

If  $|\text{deriv}| > 1e-6$ :

- $\text{Psat} = \text{Psat} - (\text{phiV} - \text{phiL})/\text{deriv}$

Otherwise:

- $\text{Psat} = \text{Psat} * 1.01$

```
% Update Psat
if abs(deriv) > 1e-6
    Psat = Psat - (phiV - phiL) / deriv;
else
    Psat = Psat * 1.01;
end
```

**e) Apply Physical Constraints:**

- Ensure pressure stays within physical bounds:

$$0.01 \text{ bar} \leq \text{Psat} \leq 0.99 * \text{Pc},$$

```
% Physical constraints
Psat = max(0.01, min(Psat, Pc * 0.99));
```

In order to ensure that the calculations have convergence.

- 0.99\*Pc

To avoid touching or exceeding the critical pressure, because at this point there is no longer any liquid-vapor separation, therefore no longer any defined Psat.

- 0.01 bar

By using this step, Psat won't be too close to zero, which would cause division by zero or logarithms of negative numbers in calculations

- Loop continues until either:
  - Fugacity difference (err) is less than tolerance
  - Maximum iterations reached.

#### II.4.3. Steps of calculation the molar volume.

- After running the previous code that shown in the steps of calculation the saturation pressure, we'll get the different values of the Psat.
- Using Excel worksheet, we calculate the molar volume.
- Using the equation (I.6), we get:

$$V = \frac{ZRT}{P_{sat}}$$

#### II.4.4. Steps to Calculate Enthalpy of Vaporization.

From the previous chapter in (I.10) we mention the steps of determination the residual enthalpy and the enthalpy of vaporization.

- ✚ The provided MATLAB code calculates the residual enthalpy ( $H_r$ ) for both the vapor and liquid phases.
- ✚ For the enthalpy of vaporization, we use excel worksheet using the equation (I-38)

The steps of MATLAB code are:

1. Determine the Temperature Derivative of (da/dT)
2. Calculate the residual enthalpy for both phases.

This part of the code calculates the temperature derivative of the SRK parameter (da/dT) and then uses it to calculate the residual enthalpy of the vapor phase and liquid (Hr\_v, Hr\_L) based on the Soave-Redlich-Kwong (SRK) equation of state.

```
function Hr_v = calculate_residual_enthalpy_v(T, P, Tc, Pc, w, Zv)
    R = 0.08314472; % bar.L/mol.K

    % Calculate SRK parameters
    Tr = T / Tc;
    omega = 0.48 + 1.574 * w - 0.176 * w^2;
    alpha = (1 + omega * (1 - sqrt(Tr)))^2;
    a = 0.42748 * (R^2) * (Tc^2) / Pc * alpha;
    b = 0.08664 * R * Tc / Pc;
    B = b * P / (R * T);

    % Calculate da/dT using the equation from the image
    da_dT = -0.42748 * (R^2 * Tc / Pc) * (1 + omega * (1 - sqrt(Tr))) * omega /
    sqrt(Tr);

    % Calculate residual enthalpy using the equation from the image
    % HR = RT(Z-1) + (T(da/dT) - a)/b * ln((Z + B)/Z)
    Hr_v = R * T * (Zv - 1) + (T * da_dT - a) / b * log((Zv + B) / Zv);
end
```

**Figure II-10:** Residual Enthalpy Calculation for Vapor Phase Using SRK EOS.

- ✚ This part of code is only for the vapor phase, the same process for the liquid.
- ✚ Next, we use the results to calculate the enthalpy of vaporization.

#### II.4.5. Results and plotting

- ✚ After applying the procedures explained above, our MATLAB code was executed, and the obtained results are presented in this section.

### 1. Results of calculation the saturation pressure.

The results show the saturation pressure (Psat) and fugacity coefficients (phiV, phiL) of ethylene (C<sub>2</sub>H<sub>4</sub>) calculated (SRK EOS).

**Table II-1:** Results of calculation the saturation pressure

T_K	Psat_bar	phiV	PhiL	Psat NIST
120	0.01358	0.99912	0.99912	0.013683
130	0.04367	0.99766	0.99766	0.044241
140	0.11675	0.99478	0.99478	0.1185
150	0.26984	0.98984	0.98984	0.27377
160	0.55533	0.98224	0.98224	0.56235
170	1.04065	0.97151	0.97151	1.0509
180	1.80667	0.95736	0.95736	1.8184
190	2.94531	0.93973	0.93973	2.9541
200	4.55712	0.91873	0.91873	4.5548
210	6.74894	0.89461	0.89461	6.7231
220	9.63210	0.86775	0.86775	9.5662
230	13.32095	0.83858	0.83858	13.196
240	17.93192	0.80755	0.80755	17.73
250	23.58287	0.77512	0.77512	23.295
260	30.39281	0.74173	0.74173	30.035
270	38.48182	0.70778	0.70778	38.125

This table shows the results of the saturation pressure (Psat) calculations at different temperatures (in Kelvin), compared to the reference values from NIST. It also includes the fugacity coefficients for the vapor phase (phiV) and the liquid phase (PhiL).

- The saturation pressure (Psat) increases significantly with temperature, rising from 0.01358 bar at 120 K to 38.48182 bar at 270 K.
- The calculated Psat values using the SRK EOS show very good agreement with the NIST reference data.
- At low temperatures, PhiV and PhiL are close to 1, meaning the system behaves almost ideally.
- As the temperature rises, these values deviate from 1, indicating non-ideal behavior.

### 1.1. Plotting The PV diagram for both the calculation and experimental results.

- ✚ This diagram represents the saturation pressure as a function of molar volume for both SRK results and the NIST.

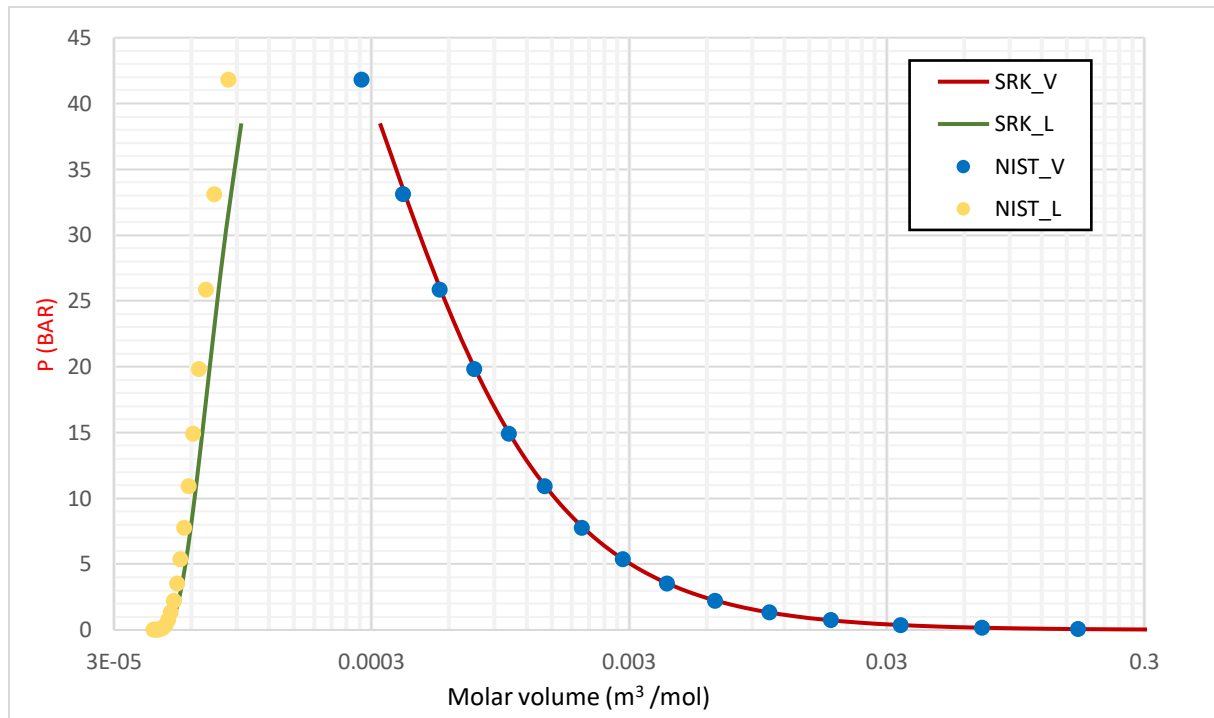


**Figure II-11:** PV diagram of the calculation and experimental results.

- The liquid phase data are clustered at much lower molar volumes, with both SRK and NIST showing a nearly vertical trend, indicating very low compressibility of the liquid phase
- The SRK EOS matches the NIST experimental vapor phase data quite well across the entire range of molar volumes and pressures. This suggests that the SRK EOS provides a good approximation for the vapor phase of ethylene under these conditions.
- The SRK EOS also aligns closely with the NIST experimental liquid phase data at low molar volumes, though the match is not perfect.

### 2. Results of calculation the molar volume.

- The table II.13 presents the calculated molar volumes for two phases using the (SRK) EOS.
- This table provides compressibility factors ( $Z$ ) and molar volumes ( $V$ ) for both vapor and liquid phases of ethylene across a temperature range from 120 K to 270 K, using (SRK EOS).

**Table II-2:** Results of calculation the compressibility factor and molar volume.

T_K	Z <sub>v</sub>	Z <sub>l</sub>	V <sub>v</sub> (m <sup>3</sup> /mol)	V <sub>v</sub> NIST	V <sub>l</sub> (m <sup>3</sup> /mol)	V <sub>l</sub> NIST
120	0.999114	6.28E-05	0.73379	0.72821	4.6115E-05	4,42E-05
130	0.997652	0.00019	0.24689	0.24351	4.6948E-05	4,52E-05
140	0.994755	0.00048	0.09918	0.097558	4.7869E-05	4,61E-05
150	0.989743	0.001058	0.04574	0.044969	4.8892E-05	4,72E-05
160	0.981934	0.002089	0.02352	0.023142	5.0036E-05	4,83E-05
170	0.970708	0.003779	0.01318	0.012992	5.1324E-05	4,95E-05
180	0.955546	0.006372	0.00792	0.0078169	5.2784E-05	5,08E-05
190	0.936022	0.010153	0.00502	0.0049704	5.4454E-05	5,22E-05
200	0.911781	0.015453	0.00333	0.0033029	5.6386E-05	5,38E-05
210	0.882488	0.022672	0.00228	0.002273	5.8652E-05	5,56E-05
220	0.847771	0.032309	0.00161	0.0016074	6.1353E-05	5,76E-05
230	0.807124	0.045033	0.00116	0.00116	6.4644E-05	6,00E-05
240	0.759768	0.061805	0.00085	0.00084841	6.8773E-05	6,29E-05
250	0.704355	0.084158	0.00062	0.00062383	7.4174E-05	6,65E-05
260	0.638249	0.114908	0.00045	0.00045585	8.1727E-05	7,13E-05
270	0.555039	0.160635	0.00032	0.00032322	9.3704E-05	7,87E-05

The table II-2 presents the results of the calculations of the compressibility factor and molar volume for the vapor and liquid phases of ethylene at different temperatures. The results are compared with reference data from NIST.

- Z<sub>v</sub>(vapor) starts very close to 1 at low temperatures (0.999114 at 120 K), indicating that the vapor behaves nearly like an ideal gas in this range.
- As the temperature increases, Z<sub>v</sub> decreases (0.555 at 270) K. This reflects a growing deviation from ideal gas behavior.
- Z<sub>l</sub> (liquid) remains extremely low across the entire temperature range (from 6.28E-05 to 0.1606), which is typical for liquids. This suggests they are far from behaving like an ideal gas.
- As the temperature increases, V<sub>v</sub> decreases significantly, reaching 0.00032 m<sup>3</sup>/mol at 270 K. This means that the vapor becomes increasingly dense
- The molar volume of the liquid (V<sub>l</sub>) increases slightly with temperature (from 4.6115E-05 m<sup>3</sup>/mol to 9.3704E-05 m<sup>3</sup>/mol), which reflects the normal thermal expansion behavior of a liquid.
- The calculated molar volumes are very close to the NIST data, which shows that the SRK EOS is reliable.

### 3. Results of calculation the residual enthalpy.

✚ This table presents calculated values for the residual enthalpy of ethylene in both vapor (Hr\_V) and liquid (Hr\_l) phases, along with the enthalpy of vaporization ( $\Delta H_{\text{vap}}$ ) at different thermodynamic states. All values are in J/mol.

**Table II-3:**Results of calculation the residual enthalpy.

<b>T_K</b>	<b>Hr_V (J/mol)</b>	<b>Hr_l (J/mol)</b>	<b><math>\Delta H_{\text{vap}}</math></b>	<b><math>\Delta H_{\text{vap}}</math> NIST</b>
130	-6.200573	-14974.5397	14968.33908	14981
150	-32.041533	-14375.7667	14343.72513	14259
170	-106.45734	-13751.4423	13644.98498	13501
190	-267.39126	-13078.6706	12811.27935	12631
210	-560.67347	-12325.3056	11764.6321	11585
230	-1047.6362	-11439.8648	10392.22864	10274
250	-1835.3597	-10321.4494	8486.089773	8530
270	-3226.1055	-8671.34102	5445.235548	5834

This table presents the results of the calculation of residual enthalpy for the both phases (Hr\_v), (Hr\_l), and the enthalpy of vaporization ( $\Delta H_{\text{vap}}$ ), along with a comparison to NIST reference values.

- For each temperature, the value of Hr\_V is significantly more negative than that of Hr\_L. This suggests that the deviations from ideality in terms of enthalpy are much more important in the vapor phase than in the liquid phase. The impact of intermolecular interactions on enthalpy is more pronounced in the vapor phase
- Hr\_V decreases (becomes more negative) as you move down the table (-6.20 to -3226.10), indicating increasing deviation from ideal gas behavior at higher pressures.
- Hr\_l also becomes more negative, but at a slower rate compared to Hr\_V.
- The enthalpy of vaporization decreases significantly with increasing temperature from 14968 J/mol to 5445 J/mol
- It can be observed that the calculated values of  $\Delta H_{\text{vap}}$  are in very good agreement with the NIST data.

## II.5.PR EOS Performances Evaluation.

The Peng-Robinson (PR) equation of state is widely used to model the thermodynamic behavior of real gases, developed to improve the prediction of phase equilibria and volumetric

properties, the PR equation incorporates a correction to the attraction term that accounts for the acentric factor, offering enhanced accuracy for hydrocarbons and other non-ideal compounds. This study focuses on the calculation methods based on the PR equation as well as the graphical representation of isotherms (pressure versus molar volume), which visually illustrate non-ideal effects, phase transitions, and near-critical behavior. The goal is to provide a deeper understanding of PVT properties essential for the analysis and design of industrial processes.

### II.5.1. PR EOS Parameterization Steps.

- ✚ Using MATLAB, we calculate the PR parameters.
- ✚ The same procedure used with the Soave-Redlich-Kwong (SRK) equation was applied here, but with the Peng-Robinson (PR) equation replacing the SRK model.

### II.5.2. Steps of calculation of Saturation Pressure, Molar Volume, and Enthalpy of Vaporization.

- ✚ Using the same process with the same steps with SRK EOS we calculate:  
( $P_{\text{sat}}$ ,  $V_L$ ,  $V_v$ ,  $H_{R\_V}$ ,  $H_{R\_L}$ )
- ✚ The only difference is in the equations used.

#### 1- PR EOS & Compressibility Factor (Z):

Solve cubic equation (I-16) using Newton-Raphson Method

- Initial guess:  $Z=1$  (vapor) or  $Z=1.5$  B (liquid).
- Iterate until  $|Z_{\text{new}}-Z| < 10^{-8}$
- Apply corrections for phase consistency.

#### 2- Molar Volume Calculation:

After determining  $P_{\text{sat}}$  and  $Z$ , compute molar volume using eq (I-6)

- Implemented in Excel for given  $T$  and  $P_{\text{sat}}$

#### 3- Enthalpy of Vaporization ( $\Delta H_{\text{vap}}$ ) Calculation.

- Compute  $(da/dT)$  (temperature derivative of PR parameter using eq (I-38).
- Calculate  $H_{R\_V}$ ,  $H_{R\_L}$  using eq (I-36)
- $\Delta H_{\text{vap}}$  via Excel using eq (I-39)

### II.5.3. Results and plotting.

In this section, our calculation results, and their comparative plotting, will be presented, mainly the saturation pressure, molar volumes, and corresponding compressibility coefficients:

#### 1. Results of calculation the saturation pressure.

- ✚ This table presents the results of the saturation pressure ( $P_{sat}$ ) calculation as a function of temperature ( $T_K$ ) and the  $P_{sat\_NIST}$ , using the Peng-Robinson (PR) equation of state. It also shows the fugacity coefficients in the vapor phase ( $\phi_V$ ) and in the liquid phase ( $\phi_L$ ) for each temperature.

**Table II-4:**Results of calculation the saturation pressure with PR

T_K	Psat_bar	phiV	phiL	Psat NIST
120	0.0156	0.9990	0.9990	0,013683
130	0.0484	0.9974	0.9974	0,044241
140	0.1259	0.9943	0.9943	0,1185
150	0.2848	0.9890	0.9890	0,27377
160	0.5763	0.9810	0.9810	0,56235
170	1.0657	0.9698	0.9698	1,0509
180	1.8312	0.9550	0.9550	1,8184
190	2.9620	0.9366	0.9366	2,9541
200	4.5559	0.9147	0.9147	4,5548
210	6.7186	0.8894	0.8894	6,7231
220	9.5617	0.8611	0.8611	9,5662
230	13.2030	0.8302	0.8302	13,196
240	17.7654	0.7971	0.7971	17,73
250	23.3784	0.7623	0.7623	23,295
260	30.1783	0.7261	0.7261	30,035
270	38.3098	0.6891	0.6891	38,125

- The saturation pressure ( $P_{sat}$ ) increases significantly with temperature, rising from 0.0156 bar at 120 K to 38.3098 bar at 270 K, as the temperature increases, a higher pressure is required to reach equilibrium between the liquid and vapor phases.
- At each temperature, we observe that  $\phi_V = \phi_L$ , which confirms that the system is indeed at vapor-liquid equilibrium.
- The fugacity coefficients decrease as the temperature increases.
- The values of  $P_{sat}$  calculated with PR are very close to the NIST reference values.

### **1-1 Plotting The PV diagram for both the calculation and experimental results.**

- ✚ This diagram represents the saturation pressure as a function of molar volume for both PR results and the NIST.

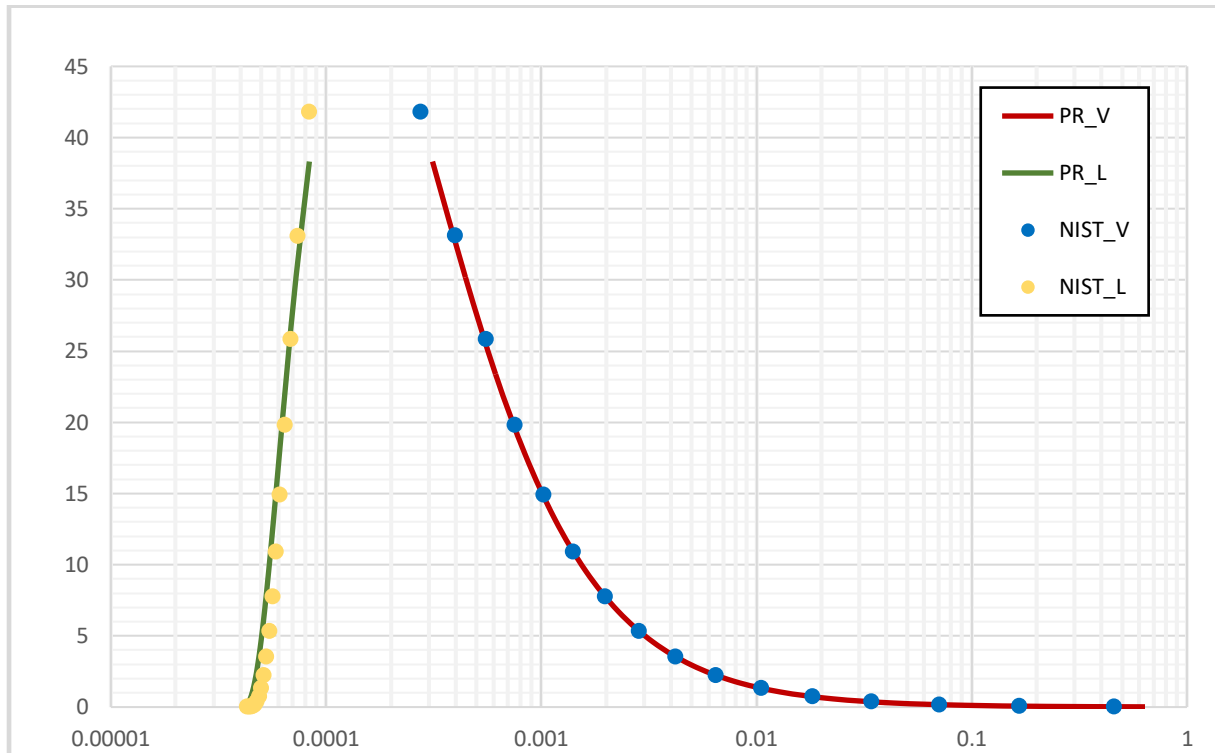


**Figure II-12:** PV diagram of the calculation and experimental results for PR.

- For the vapor phase, both the PR calculation (PR\_V) and the NIST experimental data (NIST\_V) show excellent agreement.
- Similarly, in the liquid phase, the PR calculation (PR\_L) also shows good agreement with the NIST experimental data (NIST\_L).

### **2. Results of calculation the molar volume.**

- ✚ The table shows the variation of the molar volume (V) and the compressibility factor (Z) for ethylen in the vapor and liquid phases calculated using the Peng-Robinson equation of state, along with a comparison to NIST reference values

**Table II-5:**Results of calculation the molar volume with PR

Z <sub>v</sub>	Z <sub>l</sub>	V <sub>v</sub>	V <sub>l</sub>	V <sub>v</sub> nist	V <sub>l</sub> nist
0.998972	0.000064	0.638784	4.1054E-05	0,72821	4,42E-05
0.997356	0.000187	0.222642	4.1752E-05	0,24351	4,52E-05
0.994224	0.000460	0.091917	4.2526E-05	0,097553	4,61E-05
0.988889	0.000991	0.043305	4.3388E-05	0,044969	4,72E-05
0.980661	0.001921	0.022638	4.4355E-05	0,023142	4,83E-05
0.968907	0.003427	0.012850	4.5447E-05	0,012992	4,95E-05
0.953081	0.005713	0.007789	4.6691E-05	0,0078169	5,08E-05
0.932724	0.009023	0.004974	4.8121E-05	0,0049704	5,22E-05
0.907433	0.013640	0.003312	4.9785E-05	0,0033029	5,38E-05
0.876822	0.019913	0.002279	5.1748E-05	0,002273	5,56E-05
0.840463	0.028285	0.001608	5.4107E-05	0,0016074	5,76E-05
0.797794	0.039360	0.001155	5.7005E-05	0,00116	6,00E-05
0.747986	0.054025	0.000840	6.0679E-05	0,00084841	6,29E-05
0.689652	0.073722	0.000613	6.5544E-05	0,00062383	6,65E-05
0.620140	0.101143	0.000444	7.2448E-05	0,00045585	7,13E-05
0.533085	0.142669	0.000312	8.3598E-05	0,00032322	7,87E-05

➤ **Evolution of the compressibility factor Z**

- The compressibility factor in the vapor phase (Z<sub>v</sub>) gradually decreases with increasing saturation pressure and temperature. It goes from 0.998972 to 0.533085, indicating that the gas increasingly deviates from ideal behavior ( $Z = 1$ ).
- At the same time, Z<sub>l</sub> (liquid phase) increases slightly, from 0.000064 to 0.142669, remaining much less than 1, this reflects the very low compressibility of the liquid, meaning its volume changes little even at higher pressure.

➤ **Evolution of the molar volume V**

- The molar volume of the vapor phase (V<sub>v</sub>) decreases sharply, from 0.638784 m<sup>3</sup>/mol to 0.000312 m<sup>3</sup>/mol, this means the vapor becomes denser (takes up less space) as temperature and pressure increase.
- The liquid molar volume (V<sub>l</sub>) increases slightly with temperature, this reflects the thermal expansion of the liquid (it takes up a little more space when heated).
- The molar volume values for both the liquid (V<sub>l</sub>) and vapor (V<sub>v</sub>) phases obtained in this study are generally in good agreement with the reference data from NIST.

### 3. Results of calculation the residual enthalpy and the enthalpy of vaporization.

- ✚ This table presents the results of the calculation of residual enthalpy for the both phases ( $H_{r\_v}$ ), ( $H_{r\_l}$ ), and the enthalpy of vaporization ( $\Delta H_{\text{vap}}$ ), along with a comparison to NIST reference values.

**Table II-6:**Results of calculation residual enthalpy and the enthalpy of vaporization with PR.

<b>T_K</b>	<b>H<sub>r_v</sub></b>	<b>H<sub>r_l</sub></b>	<b><math>\Delta H_{\text{vap}}</math></b>	<b><math>\Delta H_{\text{vap}}</math> NIST</b>
130	-6.7883543	-14534.7536	14527.9653	14981
150	-33.608453	-14014.3381	13980.7297	14259
170	-108.98936	-13464.3393	13355.3499	13501
190	-270.18192	-12862.9154	12592.7334	12631
210	-562.96905	-12178.721	11615.752	11585
230	-1049.9224	-11360.5515	10310.6291	10274
250	-1841.4264	-10306.5578	8465.13147	8530
270	-3247.7296	-8713.25843	5465.52886	5834

- The residual enthalpy of the vapor ( $H_{r\_v}$ ) becomes increasingly negative as the temperature increases (from -2.41 to -3247.73 kJ/kmol).
- As the temperature increases, the residual enthalpy of the liquid ( $H_{r\_l}$ ) becomes less negative.
- The enthalpy of vaporization decreases significantly with increasing temperature from 14,786.88 kJ/kmol to 5,465.53 kJ/kmol.
- The calculated results of ( $\Delta H_{\text{vap}}$ ) are close to the NIST values.

## II.6. Results of RMSE calculation.

- ✚ Using the equation (I-40) we calculated the RMSE of the saturation pressure for both the PR and SRK EOS.

### a. RMSE calculation for Psat

- ✚ The table II-7 shows the RMSE values for the saturation pressure that were calculated for each isotherm temperature.

**Table II-7:** RMSE results for the saturation pressure of ethylene.

<b>SRK</b>		<b>RMSE</b>	<b>PR</b>		<b>RMSE</b>
<b>P_SRK</b>	<b>P_NIST</b>		<b>P_PR</b>	<b>P_nist</b>	
0.013584	0.013683	-0.0000988	0.0156024	0.0136830	0.0019194
0.043674	0.044241	-0.0005669	0.0484169	0.0442410	0.0041759
0.116746	0.1185	-0.0017544	0.1259000	0.1185000	0.0074000
0.269836	0.27377	-0.0039342	0.2847789	0.2737700	0.0110089
0.555328	0.56235	-0.0070224	0.5762542	0.5623500	0.0139042
1.040654	1.0509	-0.0102455	1.0656926	1.0509000	0.0147926
1.806671	1.8184	-0.0117292	1.8312441	1.8184000	0.0128441
2.945315	2.9541	-0.0087854	2.9619603	2.9541000	0.0078603
4.557119	4.5548	0.0023191	4.5559026	4.5548000	0.0011026
6.748942	6.7231	0.0258425	6.7185590	6.7231000	-0.0045410
9.632101	9.5662	0.0659006	9.5617326	9.5662000	-0.0044674
13.320953	13.196	0.1249531	13.2029530	13.1960000	0.0069530
17.931919	17.73	0.2019195	17.7654121	17.7300000	0.0354121
23.582867	23.295	0.2878671	23.3784055	23.2950000	0.0834055
30.392805	30.035	0.3578053	30.1782662	30.0350000	0.1432662
38.481820	38.125	0.3568201	38.3098076	38.1250000	0.1848076
		<b>0.15811417612</b>			<b>0.031577199</b>

- At low pressures ( $P < 1$  bar): Both models show very small errors, though PR remains slightly better.
- At moderate pressures (1–10 bar): The difference becomes more noticeable, with SRK starting to diverge more.
- At high pressures ( $>20$  bar): The error in SRK increases rapidly, while PR still maintains a relatively acceptable level of accuracy.
- PR model shows much smaller deviations overall, with RMSE values generally below 0.04, even at high pressures.
- PR EOS: The low RMSE (0.0315) demonstrates that PR is highly reliable for predicting  $P_{\text{sat}}$  of ethylene. Its predictions are very close to experimental results, with only minor deviations.
- SRK EOS: The higher RMSE (0.1581) indicates that while SRK can be used for rough estimates, it is less accurate, especially at higher pressures where the deviation increases.
- The PR EOS provides a much lower RMSE than SRK for ethylene's saturation pressure, meaning it matches the experimental data more closely.

- The SRK EOS, while still reasonable, shows larger and more systematic deviations from the NIST data.

#### b. RMSE calculation for the molar volume.

- ✚ The tables II.8 & 9 compare the Soave-Redlich-Kwong (SRK) and Peng-Robinson (PR) equations of state in predicting ethylene's molar volume against NIST experimental data.

**Table II-8:** Results of RMSE calculation for the molar volume of ethylene with SRK EOS.

SRK		NIST	NIST		
V <sub>v</sub>	V <sub>1</sub>	V <sub>v</sub> NIST	V <sub>1</sub> NIST	RMSE V	RMSE L
0.73379	4.612E-05	0.72821	4.42E-05	5.58E-03	1.88E-06
0.24689	4.695E-05	0.24351	4.52E-05	3.38E-03	1.79E-06
0.09918	4.787E-05	0.09755	4.61E-05	1.62E-03	1.73E-06
0.04574	4.889E-05	0.04497	4.72E-05	7.74E-04	1.71E-06
0.02352	5.004E-05	0.02314	4.83E-05	3.79E-04	1.74E-06
0.01318	5.132E-05	0.01299	4.95E-05	1.92E-04	1.83E-06
0.00792	5.278E-05	0.00782	5.08E-05	9.82E-05	1.98E-06
0.00502	5.445E-05	0.00497	5.22E-05	4.98E-05	2.22E-06
0.00333	5.639E-05	0.00330	5.38E-05	2.40E-05	2.56E-06
0.00228	5.865E-05	0.00227	5.56E-05	9.98E-06	3.05E-06
0.00161	6.135E-05	0.00161	5.76E-05	2.47E-06	3.71E-06
0.00116	6.464E-05	0.00116	6.00E-05	-1.38E-06	4.62E-06
0.00085	6.877E-05	0.00085	6.29E-05	-2.98E-06	5.89E-06
0.00062	7.417E-05	0.00062	6.65E-05	-3.04E-06	7.70E-06
0.00045	8.173E-05	0.00046	7.13E-05	-1.91E-06	1.04E-05
0.00032	9.370E-05	0.00032	7.87E-05	5.54E-07	1.50E-05
				0.0017	5.62E-06

- The Root Mean Square Error (RMSE<sub>V</sub>) quantifies deviations:

*For SRK:*

- RMSE<sub>V</sub> ranges from 0.0058 (largest error) to  $5.54 \times 10^{-7}$  (smallest error).
- Errors decrease as molar volume decreases (better accuracy at higher pressures).
- SRK has smaller absolute errors across most conditions, especially at intermediate pressures.
- The small RMSE<sub>V</sub> values suggest that the SRK equation of state provides a reasonably accurate prediction of ethylene's molar volume compared to NIST data, especially in high-pressure conditions where errors are minimal.

**Table II-9:** Results of RMSE calculation for the molar volume of ethylene with PR EOS.

PR		NIST	NIST		
V_v	V_L	V_V nist	V_L nist	RMSE_V	RMSE_L
0.63878	4.1054E-05	0.72821	4.42E-05	-8.94E-02	-3.18E-06
0.22264	4.1752E-05	0.24351	4.52E-05	-2.09E-02	-3.41E-06
0.09192	4.2526E-05	0.09755	4.61E-05	-5.64E-03	-3.61E-06
0.04331	4.3388E-05	0.04497	4.72E-05	-1.66E-03	-3.79E-06
0.02264	4.4355E-05	0.02314	4.83E-05	-5.04E-04	-3.94E-06
0.01285	4.5447E-05	0.01299	4.95E-05	-1.42E-04	-4.05E-06
0.00779	4.6691E-05	0.00782	5.08E-05	-2.82E-05	-4.11E-06
0.00497	4.8121E-05	0.00497	5.22E-05	3.96E-06	-4.12E-06
0.00331	4.9785E-05	0.00330	5.38E-05	9.02E-06	-4.04E-06
0.00228	5.1748E-05	0.00227	5.56E-05	5.58E-06	-3.86E-06
0.00161	5.4107E-05	0.00161	5.76E-05	3.35E-07	-3.54E-06
0.00116	5.7005E-05	0.00116	6.00E-05	-4.53E-06	-3.02E-06
0.00084	6.0679E-05	0.00085	6.29E-05	-8.29E-06	-2.21E-06
0.00061	6.5544E-05	0.00062	6.65E-05	-1.07E-05	-9.31E-07
0.00044	7.2448E-05	0.00046	7.13E-05	-1.16E-05	1.15E-06
0.00031	8.3598E-05	0.00032	7.87E-05	-1.09E-05	4.88E-06
				0.023	3.52E-06

For PR:

- RMSE\_V ranges from -0.0894 (largest error, underestimation) to  $3.96 \times 10^{-6}$  (smallest error).
- Errors are larger at high molar volumes but improve significantly at smaller volumes.
- PR shows larger deviations at low pressures but improves as pressure increases.
- PR's tendency to underestimate V\_V suggests it may be more conservative in volume predictions.

➤ The Root Mean Square Error (RMSE\_L) quantifies deviations:

For SRK:

- RMSE\_L ranges from  $1.88 \times 10^{-6}$  (smallest) to  $1.50 \times 10^{-5}$  (largest).
- Errors increase slightly at lower pressures but remain small.
- SRK tends to overestimate liquid volume (predicts a less dense liquid than reality).

For PR:

- RMSE\_L ranges from  $-3.18 \times 10^{-6}$  (largest negative) to  $4.88 \times 10^{-6}$  (largest positive).

- Errors increase slightly at lower pressures but remain small.

**c. RMSE calculation for the enthalpy of vaporization.**

- ✚ The table II-10 presents enthalpy of vaporization ( $\Delta H_{\text{vap}}$ ) values for ethylene at various temperatures (120 K to 270 K) computed using both (SRK\_PR) EOS.

**Table II-10:** Results of RMSE calculation for the enthalpy of vaporization of ethylene.

SRK			PR	
$\Delta H_{\text{vap}}$	RMSE	$\Delta H_{\text{vap}}$ Experimental	$\Delta H_{\text{vap}}$	RMSE
14968.3	-12.661	14981	14527.965	-453.035
14343.7	84.725	14259	13980.730	-278.270
13645	143.985	13501	13355.350	-145.650
12811.3	180.279	12631	12592.733	-38.267
11764.6	179.632	11585	11615.752	30.752
10392.2	118.229	10274	10310.629	36.629
8486.09	-43.910	8530	8465.131	-64.869
5445.236	-388.764	5834	5465.529	-368.471
	<b>180.237</b>			<b>236.543</b>

- SRK shows a lower RMSE (180.237) compared to PR (236.543), indicating that SRK provides a closer match to experimental data overall.
- RMSE values vary significantly with temperature, particularly at low temperatures.
- At lower temperatures (120–150 K), both models show large negative RMSEs (e.g., PR at 120 K: -453.035), suggesting significant overestimation of vaporization enthalpy.
- Mid-temperature range (160–210 K) shows better agreement with experimental values for both models.
- At higher temperatures (above 240 K), RMSE values again become strongly negative, indicating decreasing model accuracy.
- The SRK model's errors fluctuate but stay more moderate than those of PR.
- The PR model shows larger systematic underestimation at low temperatures and higher fluctuation overall.
- Both SRK and PR equations of state can be used to estimate the enthalpy of vaporization of ethylene, but their accuracy is temperature-dependent.
- SRK model performs better overall, especially in the middle temperature range (180–220 K), with a lower RMSE and smaller fluctuations in error.

- PR model, while widely used, may require correction factors or modified parameters to improve accuracy at low and high temperature extremes for ethylene.

#### **d. Results interpretation.**

The SRK EOS demonstrates a higher RMSE (0.158) for saturation pressure ( $P_{\text{sat}}$ ) compared to PR, particularly at elevated pressures ( $>20$  bar), where deviations grow significantly. This aligns with SRK's original formulation, which focused on improving vapor-liquid equilibrium (VLE) predictions for hydrocarbons by introducing a temperature-dependent alpha ( $\alpha$ ) function. [13]

While SRK performs well at low pressures ( $<1$  bar), its errors increase under high-pressure conditions, reflecting its empirical fitting for the acentric factor ( $\omega$ ) and its weaker accuracy for dense phases.

For molar volume, SRK shows better agreement with experimental vapor-phase data (RMSE\_V: 0.0017) compared to PR, as its functional form was optimized for gas-phase properties. However, it slightly overestimates liquid volumes (RMSE\_L:  $5.62 \times 10^{-6}$ ), a known limitation of the model [13]

In enthalpy of vaporization ( $\Delta H_{\text{vap}}$ ), SRK achieves a lower RMSE (180.2) than PR, particularly in the mid-temperature range (180–220 K). This is attributed to SRK's thermodynamic consistency in energy-related predictions, a key focus of its development. However, errors increase at extreme temperatures, where the alpha function's empirical nature becomes less reliable.

The PR EOS yields a significantly lower RMSE (0.032) for  $P_{\text{sat}}$  across all pressure ranges, including high-pressure conditions ( $>20$  bar). This improvement stems from PR's modified attractive term and volume translation, which were specifically designed to enhance accuracy for non-polar and slightly polar compounds like ethylene [14]. Unlike SRK, PR maintains reliability even at high pressures, making it preferable for industrial applications requiring precise  $P_{\text{sat}}$  predictions.

For molar volume, PR exhibits larger deviations in vapor-phase predictions (RMSE\_V: 0.023) compared to SRK, particularly at low pressures. However, its liquid volume accuracy (RMSE\_L:  $3.52 \times 10^{-6}$ ) is competitive, owing this to its volume correction term—a deliberate enhancement over SRK (Peng & Robinson, 1976).

In  $\Delta H_{\text{vap}}$ , PR shows a higher RMSE (236.5) than SRK, with systematic underestimations at low and high temperatures. This reflects PR's prioritization of density and pressure accuracy over enthalpy calculations, a trade-off inherent in its design [14].

**Table II-11:** Comparative Performance of SRK and PR Equations of State for Key Thermodynamic Properties.

	SRK	PR EOS
<b>Saturation Pressure</b>	-	+
<b>Liquid Density</b>	-	+
<b>Vapor Density</b>	+	-
<b>Vaporization Enthalpy</b>	+	-

(+): Best Performances      (-): Lower Performances

The comparative analysis reveals that each equation of state (EOS) exhibits distinct strengths depending on the thermodynamic property of interest. The PR EOS proves to be the better choice for predicting saturation pressure ( $P_{\text{sat}}$ ) at high pressures, and liquid density, thanks to its refined volume corrections and improved performance near the critical region. In contrast, the SRK EOS demonstrates greater reliability for modeling vapor-phase properties and accurately calculating the enthalpy of vaporization ( $\Delta H_{\text{vap}}$ ), due to its stronger thermodynamic consistency in enthalpy predictions.

These observations are consistent with the historical development of both models: the PR EOS was introduced to overcome SRK's known limitations in liquid density prediction, making it more suitable for high-pressure vapor-liquid equilibrium (VLE) scenarios.

# *General Conclusion*

In our study, the core objective was to determine which of these models more accurately predicts key VLE properties namely, saturation pressure, compressibility factors, molar volumes, and enthalpy of vaporization—across a wide temperature range, by comparison with reliable experimental data from the NIST database. In pursuit of this, we applied both SRK and PR EOS in detailed computational frameworks using MATLAB, evaluated the outputs using graphical and numerical analyses, and validated the predictions through statistical metrics, especially the Root Mean Square Error (RMSE).

The comparative results of this study indicate that, both models offer reasonable accuracy in predicting the vapor–liquid behavior of ethylene under subcritical conditions, especially at lower temperatures.

The SRK equation, while simpler in form and computationally more efficient, exhibits increasing deviation from experimental values at higher pressures and temperatures. Its predictions for saturation pressures and enthalpies of vaporization are reasonably accurate at lower temperatures but tend to drift at elevated thermodynamic states.

The PR equation consistently yields predictions that are closer to experimental values across all temperature ranges considered. It shows a better fit in both vapor and liquid phase molar volumes, and provides superior estimations of residual enthalpy and enthalpy of vaporization.

The results checked by PV diagrams and saturation pressure plots, where PR predictions show tighter alignment with the NIST reference data, particularly in the superheated and near-critical regions. Additionally, the compressibility factors and calculated molar volumes derived from PR better capture the non-idealities exhibited by real ethylene, especially as the system approaches its critical point.

Quantitatively, this advantage is clearly reflected in the RMSE values: PR yielded an RMSE of 0.0315 for saturation pressure compared to 0.1581 for SRK, affirming its superior predictive performance.

Importantly, both equations facilitated effective estimation of enthalpy of vaporization through the calculation of residual enthalpies. The calculated  $\Delta H_{\text{vap}}$  values for both models followed the expected thermodynamic trend of decreasing enthalpy with increasing temperature. However, PR EOS again proved more reliable, producing  $\Delta H_{\text{vap}}$  values with lower deviations from the experimental NIST values.

The evidence clearly supports the Peng–Robinson equation of state as the more robust and reliable model for the conditions examined. Its improved formulation yields lower prediction errors and better alignment with experimental data across a wide temperature range.

This work carries practical value for process engineers and designers, while the SRK EOS may still be preferred in scenarios prioritizing computational simplicity particularly for light gases at moderate pressures—the PR EOS should be the default choice in rigorous process simulations involving ethylene and similar hydrocarbons.

Ultimately, this study underscores the importance of selecting the appropriate EOS model based on the target application's pressure-temperature range and required precision. By quantifying and validating the performance of both models, we provide a data-driven basis for informed selection of thermodynamic models in the petrochemical industry.

To build upon this work, it is recommended to extend the study to other relatively similar pure substances, such as Ethane or Propylene, to assess the performance of cubic EOS for such molecules, in order to investigate the effect, of unsaturation for former, and/or the number of carbon atom for the latter.

# *Bibliography*

- 
- [1] R. E. S. CLAUS BORGNAKKE, FUNDAMENTALS OF THERMODYNAMICS, United States of America: Don Fowley, 2009.
- [2] D. P. V. J. Kevin D. Dahm, Fundamentals of Chemical Engineering Thermodynamics, United States: Timothy Anderson, 2015.
- [3] T. Matsoukas, Fundamentals of Chemical Engineering Thermodynamics, The United States: PRENTICE HALL, 2013.
- [4] N. D. NEVERS, PHYSICAL AND CHEMICAL EQUILIBRIUM FOR CHEMICAL ENGINEERS, Canada: John Wiley & Sons, Inc., 2012.
- [5] A. DANESH, PVT AND PHASE BEHAVIOUR OF PETROLEUM RESERVOIR FLUIDS, vol. 47, Scotland: Elsevier , 1998.
- [6] I. Urieli, Engineering Thermodynamics - A Graphical Approach, Athens: Ohio University , 2021.
- [7] M. A. YUNUS A., THERMODYNAMICS AN ENGINEERING APPROACH, New York: McGraw-Hill Education., 2015.
- [8] A.E, "mychemengmusings.wordpress," 6 July 2019. [Online]. Available: <https://mychemengmusings.wordpress.com/2019/07/06/vapor-pressure-from-acentric-factor-omega-plus-corresponding-states-principle/>.
- [9] S. N. S. MAYA B. MANE, "Vapor liquid equilibria: A review," *Sci. Revs. Chem. Commun.*, vol. 2, no. 2, p. 158–171, 2012.
- [10] K. I. AL-MALAH, "RK-, SRK-, & SRK-PR-TYPE EQUATION OF STATE FOR," *Journal of Applied Chemical Science International*, vol. 2, no. 2, pp. 65-74, 2015.
- [11] M. C. G. K. a. S. V. D. K. Sharma, "Deep learning applications for disease diagnosis," in *Deep learning for medical applications with unique data*, V. B. S. a. G. R., Ed., Academic Press HALL, 2022, pp. 31-51.
- [12] "webbook.nist.gov," Standard Reference Data Act., [Online]. Available: <https://webbook.nist.gov/chemistry/fluid/>.

- [13] G. Soave, "Equilibrium Constants from a Modified Redlich-Kwong Equation of State," *Chemical Engineering Science*, vol. 27, no. 6, p. 1197–1203, 1972.
- [14] A. N. T.-C. E. o. State, "Ding-Yu Peng and Donald B. Robinson," *Industrial & Engineering Chemistry Fundamentals*, vol. 15, no. 1, p. 59–64, 1976.

# *Appendix*

**A. NIST Experimental data for liquid Ethylene at 110 < T < 280**

T (K)	P (bar)	Density (mol/m <sup>3</sup> )	Volume (m <sup>3</sup> /mol)	Internal Energy (kJ/mol)	Enthalpy (kJ/mol)	Entropy (J/mol*K)	Phase
120	0.0137	22606	4.42E-05	-3.343	-3.343	-23.306	Liquid
130	0.0442	22143	4.52E-05	-2.664	-2.664	-17.867	Liquid
140	0.1185	21673	4.61E-05	-1.987	-1.987	-12.853	Liquid
150	0.2738	21195	4.72E-05	-1.313	-1.311	-8.198	Liquid
160	0.5624	20706	4.83E-05	-0.638	-0.636	-3.848	Liquid
170	1.0509	20203	4.95E-05	0.037	0.042	0.248	Liquid
180	1.8184	19684	5.08E-05	0.717	0.726	4.133	Liquid
190	2.9541	19144	5.22E-05	1.403	1.418	7.844	Liquid
200	4.5548	18579	5.38E-05	2.099	2.123	11.417	Liquid
210	6.7231	17983	5.56E-05	2.809	2.846	14.885	Liquid
220	9.5662	17348	5.76E-05	3.537	3.592	18.279	Liquid
230	13.1960	16660	6.00E-05	4.289	4.369	21.637	Liquid
240	17.7300	15902	6.29E-05	5.075	5.187	24.999	Liquid
250	23.2950	15043	6.65E-05	5.907	6.062	28.425	Liquid
260	30.0350	14025	7.13E-05	6.811	7.025	32.018	Liquid
270	38.1250	12704	7.87E-05	7.844	8.144	36.011	Liquid

**B. NIST Experimental data for vapor phase of Ethylene at 110 < T < 280**

T (K)	P (bar)	Density (mol/m <sup>3</sup> )	Volume (m <sup>3</sup> /mol)	Internal Energy (kJ/mol)	Enthalpy (kJ/mol)	Entropy (J/mol*K)	Phase
120	0.0137	1.3732	7.28E-01	11.019	12.015	104.680	Vapor
130	0.0442	4.1066	2.44E-01	11.264	12.341	97.555	Vapor
140	0.1185	10.251	9.76E-02	11.505	12.661	91.775	Vapor
150	0.2738	22.238	4.50E-02	11.741	12.972	87.021	Vapor
160	0.5624	43.212	2.31E-02	11.968	13.269	83.059	Vapor
170	1.0509	76.969	1.30E-02	12.185	13.550	79.707	Vapor
180	1.8184	127.93	7.82E-03	12.390	13.811	76.829	Vapor
190	2.9541	201.19	4.97E-03	12.579	14.047	74.314	Vapor
200	4.5548	302.76	3.30E-03	12.751	14.255	72.076	Vapor
210	6.7231	439.94	2.27E-03	12.901	14.429	70.041	Vapor
220	9.5662	622.1	1.61E-03	13.024	14.562	68.143	Vapor
230	13.1960	862.04	1.16E-03	13.114	14.645	66.317	Vapor
240	17.7300	1178.7	8.48E-04	13.161	14.665	64.492	Vapor
250	23.2950	1603	6.24E-04	13.146	14.599	62.572	Vapor
260	30.0350	2193.7	4.56E-04	13.035	14.404	60.401	Vapor
270	38.1250	3093.9	3.23E-04	12.747	13.980	57.625	Vapor

## C. Table A.1: Properties of Pure Compounds.

Table A.1 (Cont.).  
Properties of pure compounds.

Name	MW kg/kgmol	T <sub>b</sub> K	T <sub>c</sub> K	P <sub>c</sub> MPa	v <sub>c</sub> m <sup>3</sup> /kgmol	Z <sub>c</sub>	acentric factor	Rackett Z <sub>RA</sub>	parachor **	Sp.Gr.
Ethylene	28.054	169.47	282.36	5.032	0.1291	0.2767	0.0852	0.28054	101.53	0.5000
Propylene	42.081	225.43	364.76	4.612	0.1810	0.2753	0.1424	0.27821	143.02	0.5210
1-Butene	56.107	266.9	419.59	4.020	0.2399	0.2765	0.1867	0.27351		0.6005
cis-2-Butene	56.107	276.87	435.58	4.206	0.2340	0.2717	0.2030	0.27044		0.6286
trans-2-Butene	56.107	274.03	428.63	4.103	0.2382	0.2742	0.2182	0.27212		0.6112
Propadiene	40.065	238.65	393.15	5.470	0.1620	0.2711	0.1596	0.27283		0.5997
1 2-Butadiene	54.092	284	444	4.500	0.2190	0.2670	0.2509	0.2685*		0.6576
1 3-Butadiene	54.092	268.74	425.37	4.330	0.2208	0.2704	0.1932	0.27130		0.6273
1-Pentene	70.134	303.11	464.78	3.529	0.2960	0.2703	0.2329	0.27035		0.6458
cis-2-Pentene	70.134	310.08	475.93	3.654	0.3021	0.2790	0.2406	0.2694*		0.6598
trans-2-Pentene	70.134	309.49	475.37	3.654	0.3021	0.2793	0.2373	0.2697*		0.6524
2-Methyl-1-Butene	70.134	304.3	465	3.400	0.2920	0.2568	0.2287	0.2705*		0.6563
3-Methyl-1-Butene	70.134	293.21	450.37	3.516	0.3021	0.2837	0.2286	0.2705*		0.6322
2-Methyl-2-Butene	70.134	311.71	471	3.400	0.2920	0.2535	0.2767	0.2663*		0.6683
1-Hexene	84.161	336.63	504.03	3.140	0.3540	0.2653	0.2800	0.2660*		0.6769
1-Heptene	98.188	366.79	537.29	2.830	0.4130	0.2616	0.3310	0.2615*		0.7015
Cyclopentane	70.134	322.4	511.76	4.502	0.2583	0.2733	0.1943	0.26824	210.05	0.7603
Methylcyclopentane	84.161	344.96	532.79	3.784	0.3189	0.2725	0.2302	0.2704*		0.7540
Cyclohexane	84.161	353.87	553.54	4.075	0.3079	0.2726	0.2118	0.27286	247.89	0.7835
Methylcyclohexane	98.188	374.08	572.19	3.471	0.3680	0.2685	0.2350	0.26986	289.00	0.7748
Ethylcyclopentane	98.188	376.62	569.52	3.397	0.3745	0.2687	0.2715	0.2667*		0.7712
Ethylcyclohexane	112.215	404.95	609.15	3.040	0.4500	0.2701	0.2455	0.2690*	328.74	0.7921
Benzene	78.114	353.24	562.16	4.898	0.2589	0.2714	0.2108	0.26967	210.96	0.8829
Toluene	92.141	383.78	591.79	4.109	0.3158	0.2637	0.2641	0.2639*	252.33	0.8743
Ethylbenzene	106.167	409.35	617.17	3.609	0.3738	0.2629	0.3036	0.26186	292.27	0.8744
o-Xylene	106.167	417.58	630.37	3.734	0.3692	0.2630	0.3127	0.2620*		0.8849
m-Xylene	106.167	412.27	617.05	3.541	0.3758	0.2594	0.3260	0.2620*		0.8694
p-Xylene	106.167	411.51	616.26	3.511	0.3791	0.2598	0.3259	0.2870*		0.8666
Nitrogen	28.014	77.35	126.1	3.394	0.0901	0.2917	0.0403	0.28971	61.12	0.8094
Oxygen	31.999	90.17	154.58	5.043	0.0734	0.2880	0.0218	0.28962		1.1421
Carbon Monoxide	28.010	81.7	132.92	3.499	0.0931	0.2948	0.0663	0.28966		
Carbon Dioxide	44.010	194.67	304.19	7.382	0.0940	0.2744	0.2276	0.27275	82.00	0.8180

**عنوان المذكرة: رسم مخططات الضغط والحجم (PV)، باستخدام معادلات الحالة التكميحية (EOS)، للمادة النقية، وبعض حسابات الخصائص الديناميكية الحرارية.**

**اللقب والاسم:** مشماش خديجة، بن الشين نسبية  
**المؤطر:** بورزق محمد الطاهر

**ملخص:** يُعتبر توازن الطور بين البخار والسائل من المفاهيم الأساسية في علم الديناميكا الحرارية والهندسة الكيميائية. تُستخدم معادلتنا الحالة "بنج-روبينسون" و"سواف-ريدلك-كوانج" لنمذجة هذا السلوك لغاز الإيثيلين، وهو أحد الهيدروكربونات الخفيفة التي تلعب دورًا مهمًا في صناعة البتروكيماويات. تركز هذه الدراسة على تقييم أداء معادلات الحالة في التنبؤ بالخصائص الديناميكية الحرارية المهمة، وخاصة ضغط التشبع والحجم المولي، وذلك ضمن نطاق واسع من درجات الحرارة. كما تشمل الدراسة خاصة مهمة أخرى وهي المحتوى الحراري للتبخير. ولتحقيق هذا الهدف، تم تحليل ومقارنة تنبؤات المعادلات مع البيانات التجريبية المعتمدة من الهيئة الوطنية للمعايير والتقنية. تشير النتائج إلى أن كلا النموذجين يقدمان دقة مقبولة في التنبؤ بسلوك التوازن بين البخار والسائل في الظروف تحت الحرجة، خصوصًا عند درجات الحرارة المنخفضة. تُعد معادلة "سواف-ريدلك-كوانج" أبسط من حيث الصياغة وأكثر كفاءة من الناحية الحسابية، لكنها تُظهر انحرافًا متزايدًا عند الارتفاع في الضغط ودرجة الحرارة. بينما تكون تنبؤاتها جيدة عند درجات الحرارة المنخفضة، فإنها تصبح أقل دقة عند الظروف الديناميكية الحرارية العالية. أما معادلة "بنج-روبينسون"، فقد أظهرت دقة أعلى بشكل مستمر عند جميع درجات الحرارة. كما قدمت توافقًا أفضل في الحجم المولي للطورين البخاري والسائل، بالإضافة إلى تقديرات أدق للمحتوى الحراري للتبخير. وتثبت النتائج أن معادلة "بنج-روبينسون" أكثر قوة وموثوقية، حيث توفر أخطاء أقل في التنبؤ وتطابقًا أفضل مع البيانات التجريبية عبر نطاق واسع من درجات الحرارة.

**كلمات مفتاحية:** سواف ريدلش كوانج، بينغ روبينسون، ضغط التشبع، الحجم المولي، إنتالبي التبخير، التوازن بين الطور السائل و البخار، الإيثيلين.

**Titre du mémoire : Traçage de diagramme pression-volume (PV), en utilisant des équations d'état cubiques (EOS), pour la substance pure, et quelques calculs de propriétés thermodynamiques.**

**Nom et prénom :** MECHEMACHE Khadidja , BENCHINE Noussaiba

**Encadrant :** BOUREZG Mohammed Tahar

**Résumé :** L'équilibre liquide-vapeur (VLE) est un concept fondamental en thermodynamique et en génie chimique. Les équations d'état PR et SRK sont utilisées pour modéliser ce comportement, notamment pour l'éthylène, un hydrocarbure léger qui joue un rôle essentiel dans l'industrie pétrochimique. Notre étude se concentre sur l'évaluation des performances de ces équations d'état dans la prédiction de propriétés thermodynamiques clés, en particulier la pression de saturation, les volumes molaires, sur une plage de températures. Une autre propriété importante étudiée dans ce travail est l'enthalpie de vaporisation ( $\Delta H_{vap}$ ). Pour cela, nous avons analysé et comparé les prédictions des deux équations avec les données expérimentales issues du NIST. Les résultats comparatifs montrent que les deux modèles offrent une précision raisonnable pour prédire le comportement liquide-vapeur en conditions subcritiques, surtout à basse température. SRK, bien que plus simple et plus rapide à calculer, présente des écarts croissants à haute pression et température. Ses prédictions restent correctes à basse température, mais deviennent moins précises à des états thermodynamiques élevés. PR, quant à elle, fournit des résultats plus proches des données expérimentales sur toute la plage de températures. Elle offre un meilleur ajustement pour les volumes molaires des phases liquide et vapeur, et donne de meilleures estimations de l'enthalpie de vaporisation. Les résultats soutiennent clairement que l'équation d'état PR est un modèle plus robuste et plus fiable. Sa formulation améliorée permet de réduire les erreurs de prédiction et d'assurer une meilleure concordance avec les données expérimentales sur une large plage de températures.

**Mots clés :** SRK, PR, VLE, pression de saturation, volume molaire, enthalpie de vaporisation, Ethylène.

**Memory title: Pressure-Volume (PV) Diagrams plotting, using Cubic Equations of States (EOS), for pure substance, and some thermodynamic properties calculations.**

**Name and First name:** MECHEMACHE Khadidja, BENCHINE Noussaiba

**Directed by:** BOUREZG Mohammed Tahar

**Abstract:** VLE is a fundamental concept in thermodynamics and chemical engineering. PR and SRK EOS are employed, to model such behavior, for Ethylene, a light hydrocarbon that plays a vital role in the petrochemical industry. Our research is focused on evaluating EOS performance in predicting key thermodynamic properties, specifically, saturation pressure, molar volumes, across a range of temperatures. Another key property investigated in this work is the enthalpy of vaporization ( $\Delta H_{vap}$ ). To answer this, we analyze and compare the EOS predictions against experimental data (NIST). The comparative results indicate that, Both models offer reasonable accuracy in predicting the vap-liq behavior under subcritical conditions, especially at lower temperatures. SRK, while simpler in form and computationally more efficient, exhibits increasing deviation at higher P & T. Its predictions for are reasonably accurate at lower temperatures but tend to drift at elevated thermodynamic states. PR consistently yields predictions closer to experimental values across all T ranges. It shows a better fit in both vapor and liquid phase molar volumes, and provides superior estimations of enthalpy of vaporization. The evidence clearly supports the PR EOS as more robust and reliable model. Its improved formulation yields lower prediction errors and better alignment with experimental data across a wide temperature range

**Key words:** SRK, PR, vapor-liquid equilibrium (VLE), saturation pressure, molar volume, enthalpy of vaporization, Ethylene.